

MIT Open Access Articles

TnSmu1 is a functional integrative and conjugative element in Streptococcus mutans that when expressed causes growth arrest of host bacteria

The MIT Faculty has made this article openly available. **Please share** how this access benefits you. Your story matters.

Citation: McLellan, Lisa K, Anderson, Mary E and Grossman, Alan D. 2022. "TnSmu1 is a functional integrative and conjugative element in Streptococcus mutans that when expressed causes growth arrest of host bacteria." Molecular Microbiology.

As Published: 10.1111/mmi.14992

Publisher: Wiley

Persistent URL: <https://hdl.handle.net/1721.1/146803>

Version: Final published version: final published article, as it appeared in a journal, conference proceedings, or other formally published context

Terms of use: Creative Commons Attribution NonCommercial License 4.0



RESEARCH ARTICLE

TnSmu1 is a functional integrative and conjugative element in *Streptococcus mutans* that when expressed causes growth arrest of host bacteria

Lisa K. McLellan  | Mary E. Anderson  | Alan D. Grossman 

Department of Biology, Massachusetts Institute of Technology, Cambridge, Massachusetts, USA

Correspondence

Alan D. Grossman, Department of Biology, Building 68-530, Massachusetts Institute of Technology, Cambridge, MA 02139, USA.

Email: adg@mit.edu

Funding information

National Institute of General Medical Sciences, Grant/Award Number: R35 GM122538

Abstract

Integrative and conjugative elements (ICEs) are major drivers of horizontal gene transfer in bacteria. They mediate their own transfer from host cells (donors) to recipients and allow bacteria to acquire new phenotypes, including pathogenic and metabolic capabilities and drug resistances. *Streptococcus mutans*, a major causative agent of dental caries, contains a putative ICE, TnSmu1, integrated at the 3' end of a leucyl tRNA gene. We found that TnSmu1 is a functional ICE, containing all the genes necessary for ICE function. It excised from the chromosome and excision was stimulated by DNA damage. We identified the DNA junctions generated by excision of TnSmu1, defined the ends of the element, and detected the extrachromosomal circle. We found that TnSmu1 can transfer from *S. mutans* donors to recipients when co-cultured on solid medium. The presence of TnSmu1 in recipients inhibited successful acquisition of another copy and this inhibition was mediated, at least in part, by the likely transcriptional repressor encoded by the element. Using microscopy to track individual cells, we found that activation of TnSmu1 caused an arrest of cell growth. Our results demonstrate that TnSmu1 is a functional ICE that affects the biology of its host cells.

KEYWORDS

conjugation, horizontal gene transfer, integrative and conjugative element, mobile genetic element, *Streptococcus mutans*

1 | INTRODUCTION

Horizontal gene transfer (HGT) is a driving force in microbial evolution, allowing bacteria to acquire new traits and phenotypes from other bacterial lineages. Biofilms, including dental plaque, are hot spots for HGT, and HGT is well documented in the oral microbiome (Jones et al., 2021; Lunde et al., 2021; Olsen et al., 2013; Roberts et al., 1999, 2001). Further, oral bacteria can cause major health issues. For example, *Streptococcus mutans*, a major causative agent

of dental caries, acts as a reservoir for antibiotic resistance genes and mobile genetic elements within the oral microbiome and can be a causative agent of infective endocarditis (Lunde et al., 2021; Nomura et al., 2020; Olsen et al., 2013).

Much is known about quorum sensing and HGT through natural competence in *S. mutans* (reviewed in Shanker and Federle [2017]). Other types of HGT are mediated by mobile genetic elements that are often found integrated in the genome of the host organism. These can have a broad host range and some can mediate genetic

This is an open access article under the terms of the [Creative Commons Attribution-NonCommercial](https://creativecommons.org/licenses/by-nc/4.0/) License, which permits use, distribution and reproduction in any medium, provided the original work is properly cited and is not used for commercial purposes.

© 2022 The Authors. *Molecular Microbiology* published by John Wiley & Sons Ltd.

exchange between distantly related organisms that may be unable to exchange DNA through transformation. Conjugative elements and bacteriophage are mobile genetic elements that can mediate their own transfer from a host (donor) bacterium to a recipient.

Integrative and conjugative elements (ICEs) represent the most prevalent type of conjugative element and are found in all major clades of bacteria, including those that cause dental caries and others found in the mouth (Guglielmini et al., 2011; Lunde et al., 2021; Roberts et al., 2001; Roberts & Mullany, 2009, 2011). Integrative and conjugative elements mediate their own transfer from a host cell to a recipient and often contain cargo genes that confer beneficial phenotypes to the host cells. Phenotypes conferred by ICEs include: virulence, symbiosis, metabolic functions, and drug resistances (reviewed in Johnson and Grossman [2015]). ICEs are major contributors to the spread of antibiotic resistance determinants among multidrug-resistant pathogens and are notable in the human microbiome and other microbial communities (Botelho & Schulenburg, 2021; Jiang et al., 2019). However, fundamental aspects of ICE biology within the complex communities of dental plaque remain unknown.

Although their size, regulation, and interactions with host cells can vary considerably, ICEs generally follow a standard lifecycle (reviewed in Wozniak and Waldor [2010]; Auchtung et al. [2016]; Botelho and Schulenburg [2021]). Briefly, ICEs typically reside integrated in the chromosome of a bacterial host. Under certain conditions or perhaps stochastically, ICE gene expression becomes active and the ICE excises from the host chromosome to form an extrachromosomal circular dsDNA molecule. This is then processed by ICE- and host-encoded proteins to generate a nucleoprotein complex containing linear single-stranded ICE DNA. Element DNA (as linear ssDNA) can then be transferred to a new host through the element-encoded conjugation machinery, a type IV secretion system (T4SS). Once in the recipient, the linear ssDNA circularizes and is converted into dsDNA. The circular dsDNA can then be integrated into the recipient genome through the action of an ICE-encoded recombinase, generating a stable transconjugant (recipient that has stably acquired a copy of an ICE).

While integrated in the host chromosome, expression of most of the genes required for the ICE lifecycle is repressed (Auchtung et al., 2005, 2007; Roberts & Mullany, 2009). In many ICEs, this is controlled by a transcriptional repressor. Upon activating signals, the repressor is inactivated, sometimes via proteolytic cleavage by an element-encoded anti-repressor (Bose et al., 2008). This allows the genes required for ICE transfer to be expressed and the ICE lifecycle to continue.

Throughout its lifecycle, the interactions between an ICE and its host cell are complex. ICEs often benefit their host cells through associated cargo genes that confer specific phenotypes (mentioned above). However, ICEs can also manipulate host development, growth, and viability (Beaber et al., 2004; Bean, McLellan, & Grossman, 2022b; Jones et al., 2021; Pembroke & Stevens, 1984; Reinhard et al., 2013).

Tn*Smu1* is a putative ICE found in some isolates of the prototypic oral pathogen *S. mutans*. (Ajdic et al., 2002, p. 159; Bi et al., 2012). Tn*Smu1* was recognized bioinformatically based on comparisons to the conjugation machinery and DNA processing machinery encoded by two well-studied ICEs: Tn916, the first described ICE discovered through its ability to spread tetracycline resistance through clinical isolates of *Enterococcus* (Franke & Clewell, 1981a; Franke & Clewell, 1981b, p. 916), and ICEBs1, a well-studied ICE in *Bacillus subtilis* (Auchtung et al., 2007, 2016; Jones et al., 2021; Lee et al., 2007; Lee & Grossman, 2007).

We found that Tn*Smu1* is a functional ICE that is capable of undergoing a complete ICE life cycle. We demonstrate that Tn*Smu1* can excise from its host chromosome to form a circular dsDNA molecule, transfer to recipient cells, and integrate into the chromosome to generate stable transconjugants. Using PCR-based assays, we identified the integration site, defined the ends of the element, and detected the extrachromosomal circle. We found that DNA damage modulates the excision of Tn*Smu1*. Further, by co-culturing donors and recipients on a solid medium, we found that Tn*Smu1* can transfer from *S. mutans* donors to *S. mutans* recipients. However, the presence of Tn*Smu1* in recipients prevented successful acquisition of another copy of the element, at least in part, through a repressor-mediated immunity mechanism analogous to that of ICEBs1 (Auchtung et al., 2007; Bose et al., 2008). Using a fluorescent reporter in Tn*Smu1*, we were able to visualize individual cells in which Tn*Smu1* had become active. Most of the cells with an active element stopped growing. Together, our results illuminate the functionality of Tn*Smu1* and demonstrate that Tn*Smu1* affects the physiology of its host cells by halting host cell growth. As our work was nearing completion, an independent study identified the putative repressor of Tn*Smu1* and reported that the element can be activated to excise from the chromosome by conditional inactivation of the repressor and also by DNA damage (King et al., 2022).

2 | RESULTS

2.1 | Comparison of Tn*Smu1* to Tn916 and ICEBs1

Tn*Smu1* (Figure 1) is a putative ICE found in the prototypic oral pathogen *S. mutans* UA159 (Ajdic et al., 2002, p. 159; Bi et al., 2012). Tn*Smu1* was recognized bioinformatically based on comparisons to genes from the ICE Tn916 that are needed for formation of the conjugation machinery (a T4SS) and DNA processing (Table 1) (Ajdic et al., 2002; Roberts & Mullany, 2009, p. 916; Roberts & Mullany, 2011, p. 916).

S. mutans appears to be the primary host of Tn*Smu1*, although remnants or fragments appear to be present in other Streptococcal species. Using cblaster (Gilchrist et al., 2021) to search the NCBI BLASTp database, we found that at least 30 sequenced *S. mutans* genomes appear to contain an intact Tn*Smu1*, based on the presence of all the genes needed for a functional ICE and the presence of the

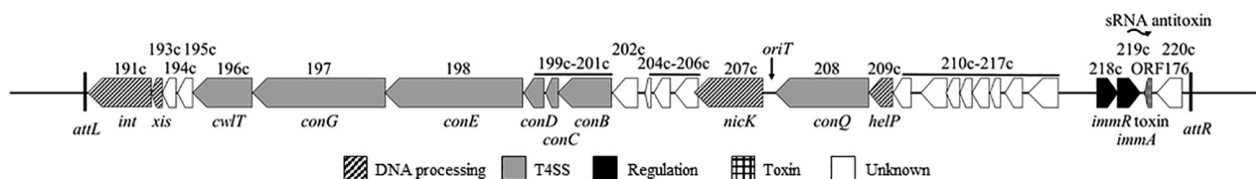


FIGURE 1 Genetic map of TnSmu1. Open reading frames are indicated by horizontal arrows. Gene names are abbreviated to include only the number designation (i.e., 191c indicates *smu_191c*). The name of the homologous ICEBs1 gene is written below. Thick vertical black lines indicate attachment sites *attL* and *attR* at the ends of TnSmu1. The putative origin of transfer (*oriT*) is indicated with a vertical arrow. Putative gene function is indicated by pattern and color: Genes of unknown function (white), genes encoding components of the type 4 secretion system (T4SS) (gray), DNA processing (diagonal stripes), and regulation (black). There is a toxin (grid pattern) and small RNA antitoxin (wavy horizontal arrow) encoded in the region between *smu_217c* and *smu_218c* (Koyanagi & Lévesque, 2013).

TABLE 1 Similarity between ICEs TnSmu1, ICEBs1, and Tn916

TnSmu1 gene ¹	Proposed name ²	% similarity (% identity) ³				Vir homolog/function/comments ⁴
		ICEBs1		Tn916		
<i>smu_191c</i>	<i>int</i>	<i>int</i>	35.8 (19.0)	<i>int</i>	37.6 (21.5)	tyrosine recombinase
<i>smu_193c</i>	<i>xis</i>	<i>xis</i>	31.6 (14.5)	<i>xis</i>	34.2 (15.1)	excisionase/recombination directionality factor
<i>smu_196c</i>	<i>cwIT</i>	<i>cwIT</i>	25.6 (17.5)	<i>orf14</i>	32.7 (19.3)	VirB1-like, cell wall hydrolase
<i>smu_197c</i>	<i>conG</i>	<i>conG</i>	26.0 (15.1)	<i>orf15</i>	29.2 (15.8)	VirB6-like, transmembrane protein
<i>smu_198c</i>	<i>conE</i>	<i>conE</i>	46.2 (28.1)	<i>orf16</i>	38.5 (22.7)	VirB4-like, AAA+ ATPase
<i>smu_199c</i>	<i>conD</i>	<i>conD</i>	33.2 (16.8)	<i>orf17</i>	24.7 (15.9)	VirB3-like, transmembrane protein
<i>smu_200c</i>	<i>conC</i>	<i>conC</i>	26.0 (12.5)	<i>orf19</i>	29.2 (19.8)	transmembrane protein
<i>smu_201c</i>	<i>conB</i>	<i>conB</i>	37.0 (21.4)	<i>orf13</i>	36.8 (18.4)	VirB8-like, transmembrane protein
<i>smu_207c</i>	<i>nickK</i>	<i>nickK</i>	40.4 (24.2)	<i>orf20</i>	46.5 (25.6)	relaxase
<i>smu_208c</i>	<i>conQ</i>	<i>conQ</i>	44.2 (26.7)	<i>orf21</i>	42.6 (26.7)	VirD4-like, AAA+ ATPase; coupling protein
<i>smu_209c</i>	<i>helP</i>	<i>helP</i>	40.8 (24.3)	<i>orf22 orf23</i>	38.3 (22.7) 30.8 (22.6)	helicase processivity factor
<i>smu_218c</i>	<i>immR</i>	<i>immR</i>	51.9 (31.3)	n/a		repressor; DNA binding protein
<i>smu_219c</i>	<i>immA</i>	<i>immA</i>	30.2 (16.1)	n/a		anti-repressor; metalloprotease, cleaves ImmR

¹TnSmu1 gene names from (Ajdic et al., 2002).

²Proposed name based on similarity to known genes. Uses ICEBs1 gene names where appropriate based on conservation (Auchtung et al., 2016).

³Calculated by EMBOSS Needle pairwise global sequence alignment (Needleman & Wunsch, 1970).

⁴Function based on similarity to characterized proteins (Auchtung et al., 2016; Fronzes et al., 2009).

regulatory genes found in TnSmu1 (Figure S1). We did not detect intact TnSmu1 in other sequenced genomes outside of *S. mutans*.

We also searched the whole genome shotgun (WGS) nucleotide collection for DNA sequences similar to TnSmu1. Parts of TnSmu1 were found in 114 of 364 sequences of *S. mutans* isolates. Of these, 30 of these sequences had >90% identity and query coverage, consistent with the analysis using cblaster. Of note, matches between TnSmu1 and DNA from bacteria outside of the Streptococci were rare and of poor query coverage ($\leq 5\%$), indicating that TnSmu1 is a *Streptococcus*-specific element. Despite the apparently limited natural host range, we suspect that TnSmu1 might readily function in other bacterial species (see Discussion).

In addition to similarity to genes in Tn916, many genes in TnSmu1 are similar to those in ICEBs1 from *B. subtilis* (Table 1) (Auchtung et al., 2016). We analyzed sequence similarities between genes in TnSmu1, ICEBs1, and Tn916 and found that TnSmu1 is predicted to

contain most, if not all of the components that are needed for the ICE lifecycle (Figure 1, Table 1).

2.1.1 | Type IV secretion system (T4SS)

We identified all the known components of the T4SS typical of Gram-positive bacteria. The membrane channel of the T4SS is likely composed of ConB, ConC, ConD, and ConG (ConB_{ICEBs1}, ConC_{ICEBs1}, ConD_{ICEBs1}, and ConG_{ICEBs1} and ORF13_{Tn916}, ORF19_{Tn916}, ORF17_{Tn916}, and ORF15_{Tn916}, for ICEBs1 and Tn916, respectively) (Auchtung et al., 2016; Ciric et al., 2013; Leonetti et al., 2015; Roberts & Mullany, 2009). All of these proteins are predicted to encode a specific number of transmembrane domains, and the approximate size of the proteins is conserved throughout T4SSs (Auchtung et al., 2016; Berkmen et al., 2010; Leonetti et al., 2015). Based on

homology or similarity, size, and predicted transmembrane localization, we predict that *smu_201c*, *smu_200c*, *smu_199c*, and *smu_197c* encode ConB_{Smu}, ConC_{Smu}, ConD_{Smu}, and ConG_{Smu}, respectively (Table 1).

ConE (ConE_{ICEBs1} and ORF16_{Tn916}) is one of two conserved ATPases found in T4SSs of Gram-positive bacteria (Auchtung et al., 2016; Fronzes et al., 2009) that are required for conjugation (Auchtung et al., 2007; Berkmen et al., 2010; Iyer et al., 2004; Leonetti et al., 2015). *smu_198c* encodes a gene product that is 46.2% similar to ConE_{ICEBs1} and 38.5% similar to ORF16_{Tn916} (Table 1), and thus we infer SMU_198c is ConE_{Smu}.

The coupling protein, ConQ_{ICEBs1} and ORF21_{Tn916}, binds the DNA protein complex (relaxosome) and "delivers" or "couples" it to the T4SS for transfer into a recipient cell. Key features of coupling proteins from T4SSs of Gram-positive bacteria include two transmembrane helices in the N-terminal domain and a C-terminal cytoplasmic ATPase domain (Alvarez-Martinez & Christie, 2009; Auchtung et al., 2016). ConQ_{Smu} (SMU_208c) shares 44.2% and 42.6% similarity with ConQ_{ICEBs1} and ORF21_{Tn916}, respectively, and is predicted to have the same structural features found in other coupling proteins (Table 1).

2.1.2 | Cell wall hydrolase

Cell wall hydrolases are critical components of conjugative elements from Gram-positive bacteria (Auchtung et al., 2016; Bhatti et al., 2013; DeWitt & Grossman, 2014). SMU_196c contains a phage tail lysozyme domain (E-value 2.20e-30 BLASTp) used by phage to degrade the cell wall peptidoglycan layer (Xiang et al., 2008). It also includes an amidase domain (E-value 1.23e-48 BLASTp). Structural predictions through Phyre2 matched the structure of SMU_196c to a cell wall hydrolase produced by *Staphylococcus aureus* (N-acetylmuramoyl-L-alanine amidase 2 from *S. aureus*, 100% confidence, 76% coverage). Therefore, we determined this is likely the cell wall hydrolase for TnSmu1 and we infer SMU_196c is CwIT_{Smu}.

2.1.3 | DNA relaxase, origin of transfer (*oriT*), and helicase processivity factor

After excision from the chromosome, the circular dsDNA is nicked and unwound for a single strand of DNA to be transferred through the T4SS. Nicking occurs at the origin of transfer (*oriT*) through the action of a DNA relaxase (or nickase) (Nick_{ICEBs1} and ORF20_{Tn916}) (Auchtung et al., 2016; Lee & Grossman, 2007; Rocco & Churchward, 2006). At least several ICEs undergo autonomous rolling-circle replication (Johnson & Grossman, 2015; Lee et al., 2010; Wright & Grossman, 2016). Like conjugation, replication initiates from *oriT* by the relaxase and also requires unwinding of the duplex DNA. In *B. subtilis*, DNA unwinding is mediated by the host-encoded DNA translocase PcrA (Lee et al., 2010; Petit et al., 1998; Thomas et al., 2013). For ICEBs1 and Tn916, a helicase processivity

factor (HelP_{ICEBs1} and ORF22 and ORF23 for Tn916) is required to facilitate DNA unwinding (Thomas et al., 2013). The genes encoding the processivity factors are immediately upstream of and in a cluster with *conQ* (coupling protein), *oriT*, and *nickK* (relaxase), in that order (Thomas et al., 2013) (Figure 1).

- (i) *nickK*_{Smu}. *smu_207c* in TnSmu1 encodes a product that is 40.4% and 46.5% similar to Nick_{ICEBs1} and ORF20_{Tn916}, respectively (Table 1). Similar to the location in ICEBs1 and Tn916, it is immediately downstream from the gene encoding the coupling protein (Figure 1). Based on the sequence similarity and location, we infer that SMU_207c is Nick_{Smu}.
- (ii) *oriT*_{Smu}. We identified a sequence in TnSmu1 that is identical in 20 of 24bp to *oriT* from ICEBs1 and Tn916 (Figure 2a) (Lee & Grossman, 2007). *oriT*_{Smu} contains an inverted repeat that is characteristic of many *oriTs* and is located just upstream of *nickK* (Figure 1). Based on the sequence and location, we infer that this is *oriT*_{Smu}.
- (iii) *helP*_{Smu}. *smu_209c* in TnSmu1 encodes a product that is 40.8% similar to the helicase processivity factor HelP_{ICEBs1} and 38.3% and 30.8% similar to ORF22 and ORF23, the two HelP homologs from Tn916 (Table 1). Additionally, it is located immediately upstream from the gene (*conQ*) that encodes the coupling protein (Figure 1). Based on the location and similarities, we infer that SMU_209c is HelP_{Smu}.

2.1.4 | Integrase and excisionase

Integrating elements typically utilize a recombinase, often called an integrase (Int), that is required for integration into and excision from a host chromosome. Integrating elements also utilize a recombination directionality factor, also called an excisionase (Xis), in combination with Int, for excision from the host chromosome (Grindley et al., 2006; Hirano et al., 2011).

smu_191c encodes a product that is 35.8% and 37.6% similar to the tyrosine recombinases (Int) encoded by ICEBs1 and Tn916, respectively (Table 1). Integrases (recombinases) are often encoded at or near an end of an ICE (Cury et al., 2017). Based on the location and protein similarities, we infer that SMU_191c is Int_{Smu}.

smu_193c encodes a gene product that is 31.6% similar and 34.2% similar to Xis_{ICEBs1} and Xis_{Tn916} (Table 1). Excisionases (Xis) are typically small, highly charged proteins often with little sequence similarity to other excisionases {e.g., (Auchtung et al., 2016; Lee et al., 2007)}. *smu_193c* encodes a small, basic protein and thus we infer that SMU_193c is likely Xis_{Smu}.

2.1.5 | Regulatory proteins (ImmA/ImmR)

TnSmu1 has two genes, *smu_218c* and *smu_219c*, that encode products similar to the repressor (ImmR) and anti-repressor and metalloprotease (ImmA) encoded by ICEBs1. SMU_218c and SMU_219c

FIGURE 2 Alignments of *oriT*, ImmR, and ImmA from Tn*Smu1*, ICEBs1, and Tn916. (a) Alignment of the putative Tn*Smu1* origin of transfer (*oriT*) to ICEBs1 and Tn916. The *nic* site of ICEBs1 and Tn916 is indicated by a vertical arrow. Inverted repeats are indicated by lines under the sequence. (b and c) Global alignments of ImmR (b) and ImmA (c) from ICEBs1 and Tn*Smu1* as calculated by EMBOSS Needle pairwise alignment (Needleman & Wunsch, 1970). “|” represents a matching amino acid; “.” represents amino acids with strongly similar properties; “:” represents amino acids with weakly similar properties; “-” represents a gap (Rice et al., 2000). (b) For ImmR, amino acids boxed in green represent a conserved helix-turn-helix motif (Bose et al., 2008; Oppenheim et al., 2005) (predicted by GYM 2.0; Narasimhan et al., 2002). Amino acids boxed in orange represent the cleavage site where ImmR_{ICEBs1} is cleaved by ImmA_{ICEBs1} (Bose et al., 2008). (c) For ImmA, amino acids boxed in blue indicate the characteristic HEXXH motif found in many zinc-dependent metalloproteases (Fujimura-Kamada et al., 1997).

(a) Origin of transfer

ICEBs1	ACCCCCCAGC	CTAACAGGGGGT
Tn916	ACCCCCGTAT	CTAACAGGGGGT
Tn <i>Smu1</i>	ACCCCCGATA	CTAATAGGGGGT

(b) ImmR

ICEBs1	MSLGKRLKEARQKAGYTQKEAAEKLNI GNNLSNYERDYRDPDPTDLLKL	
Tn <i>Smu1</i>	-MFPERLKSRLRLEAGLTQKQIAEKLEIKQQSYAQWESGRTPKRSATLNKF	
ICEBs1	SNLYNVSTDYLLGKDEVSKK-NETDLLNKTINEAIQELKDEDTLLFMND-	
Tn <i>Smu1</i>	ADFFGVTTDYLLGKTNIKKEIPEGEELEKELDRAI-----DNSVGFEGKP	
ICEBs1	-GEFDEETARLVKKALKNGIKFIDELKKKE-	127
Tn <i>Smu1</i>	VSDYDRE---VIKEVLRNYFK-----NQKNN	117

(c) ImmA

ICEBs1	VITIYTSKGIKHVKQSVIKTHGTNNVYEIC-DIQKIYI-----LKNDLG	
Tn <i>Smu1</i>	-----MNL SKIVRDTEKLGVTIIFCPFKKEKG	
ICEBs1	QANGLLQHDKATDQYLIHINENLQHQQ--FVIAHELGHYFLHKRLNTFKV	
Tn <i>Smu1</i>	-----RHLVTSNTKFILINETLSDEKINVLHEITH-FINK--DTGNI	
ICEBs1	VNCSKVLKDKLEHQASLFASELILTDKMLNEALPYIQGFSKEQIAAYFNV	
Tn <i>Smu1</i>	LSQSNFTFAHYIEKEAEV-----ERIINFMN	
ICEBs1	PSFVTDYKLSQIGSFSFNRIYSHEISAFG-----	
Tn <i>Smu1</i>	IN--DEYPIDE--SFNYLDYMHK--AFIPEKYENIVKEEAKKLYQKNKIK	
ICEBs1	-----	169
Tn <i>Smu1</i>	LTKPK	143

are 51.9% and 30.2% similar to ImmR_{ICEBs1} and ImmA_{ICEBs1}, respectively (Figure 2b,c), and we infer that the Tn*Smu1* products are ImmR_{Smu} (SMU_218c) and ImmA_{Smu} (SMU_219c). For ICEBs1, when activated, the protease ImmA cleaves ImmR to inactivate it, thereby causing de-repression of the element (Auchtung et al., 2007; Bose et al., 2008). Homologs of ImmR and ImmA are also encoded by many phages (Bose et al., 2008; Lucchini et al., 1999). ImmR_{Smu} contains a conserved a helix-turn-helix motif, a typical DNA-binding domain for phage-like repressors (Bose et al., 2008). It also has a conserved phenylalanine that may be the putative cleavage site (Figure 2b) (Bose et al., 2008). That ImmR_{Smu} acts as the repressor of Tn*Smu1* is further supported by finding that it appears essential in Tn-seq studies (Shields et al., 2018), as would be expected if deletion of the gene caused de-repression and excision of the element, thereby deleting the entire element from the chromosome. Further, ImmA_{Smu} contains a characteristic HEXXH motif found in many zinc-dependent metalloproteases (Figure 2c) (Fujimura-Kamada et al., 1997).

2.1.6 | Genes in Tn*Smu1* with unknown function

There are 15 genes in Tn*Smu1* (*smu_194c*, *smu_195c*, *smu_202c*, *smu_204c*, *smu_205c*, *smu_206c*, *smu_210c*, *smu_211c*, *smu_212c*, *smu_213c*, *smu_214c*, *smu_215c*, *smu_216c*, *smu_217c*, *smu_220c*) that lack similarity to any genes known to be needed for the ICE lifecycle. Of these, *smu_194c* is predicted to encode a protein with a DUF3850 domain (e.g. *S. mutans* DUF3850 domain-containing protein, Sequence ID: WP_019319579.1, E-value 1e-53) and has some similarity to proteins predicted to be involved in chromosome partitioning (e.g. Myoviridae sp. MAG TPA: chromosome partitioning protein, E-value 2e-20). Proteins with these properties are found in a wide range of bacterial species. *smu_194c* and *smu_195c* gene products are also similar to proteins encoded by various bacteriophage. In contrast to *smu_194c* and *smu_195c*, the other genes with unknown function in Tn*Smu1* are similar to genes found only in Streptococcal species. Based on the lack of similarity to genes or

proteins with known function, we do not have insights into the functions of the unknown genes in *TnSmu1*.

Based on the presence of the regulatory genes and the essential components of an ICE, we expected that *TnSmu1* is a functional ICE. Additionally, based on the presence of several genes of unknown function, we suspect that *TnSmu1* confers one or more phenotypes to host cells, although the nature of these phenotypes is currently not known. Below we describe experiments demonstrating that *TnSmu1* is indeed a functional element: it can excise from the host chromosome, transfer to a new host, and integrate into the chromosome of the new host to generate a stable transconjugant.

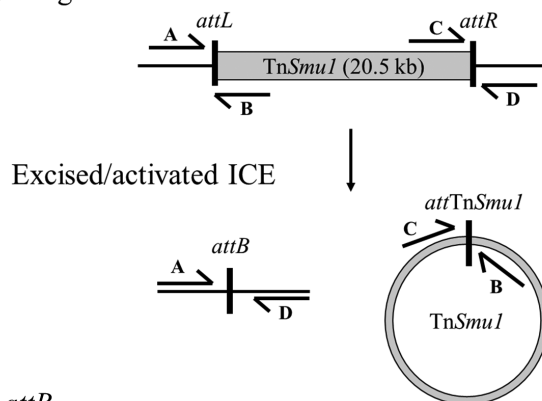
2.2 | Excision of *TnSmu1* from the host chromosome

When *TnSmu1* is integrated in the host cell chromosome, there are left and right attachment sites, *attL* and *attR*, respectively, that demarcate the junctions between *TnSmu1* and the host chromosome (Figure 3a). If capable of and upon excision, there would be a single attachment site in the element, *attTnSmu1*, where the element recombined to form an extrachromosomal circle. There would also be an attachment site in the bacterial chromosome, *attB*, that represents the fusion of chromosomal sequences that had been interrupted by insertion of the element (Figure 3a).

attL had been predicted based on the increase in A+T content throughout the element that is characteristic of horizontally acquired DNA and on the presence of nearby genes encoding putative recombinases (*smu_191c*) (Ajdic et al., 2002, p. 159; Bi et al., 2012). We noticed that *TnSmu1 attL* was in, although it did not disrupt, *smu_t33*, encoding a leucyl tRNA. ICEs are often found integrated into tRNA genes and typically do not disrupt the gene (Burrus et al., 2002; Burrus & Waldor, 2004). For example, ICEBs1 and ICEHin1056 from *B. subtilis* and *Haemophilus influenzae*, respectively, are both found integrated in a tRNA gene (Dimopoulou et al., 2002; Lee et al., 2007). The location of *attR* of *TnSmu1* had been predicted to be either after *smu_209c* or *smu_226c* (Figure 1), based on A+T content, the presence of genes encoding an integrase, relaxase, and/or type IV secretion system, and/or the presence of a large intergenic region (Ajdic et al., 2002, p. 159; Bi et al., 2012).

To test *TnSmu1* excision, we designed primer sets upstream and downstream of the predicted ends (*attL* and *attR*) that would only produce a PCR product upon excision if *attR* of *TnSmu1* was indeed after *smu_209c* or *smu_226c*. Essentially, primers located outside the element *attR* and *attL* cannot produce a PCR product when *TnSmu1* is integrated. This is due to the fact that *TnSmu1* is ~20 kb and a PCR product of this size would not be generated in the PCR conditions used. However, upon excision of *TnSmu1*, PCR of genomic DNA using primers that are outside but near the ends of the element (primers A and D in Figure 3a) should generate a readily detectable product (Figure 3a). Using genomic DNA from stationary phase cultures of *S. mutans*, we were unable to detect PCR products using these primers. This result indicates that either *TnSmu1* did not

(a) Integrated ICE



(b) *attB*

gggttcgaccc**cggccgccggtatagta**tttagctctt
ccaagctggg**gccggcgccat**atcataaatcgagaa

attTnSmu1

atagaaatat**cggccgccggtatagta**ctagcctagt
tatctttatag**gccggcgccat**atcatgatcggatca

FIGURE 3 Cartoon of *TnSmu1* inserted in the chromosome and products after excision. (a) Cartoon of *TnSmu1* inserted in the chromosome and the products after excision. A set of four primers (labeled A, B, C, D) are able to detect the junctions between the host chromosome and left (*attL*; primers A + B) and right (*attR*; primers C + D) ends of *TnSmu1*; the host attachment site without insertion of *TnSmu1* (*attB*; primers A + D) and the excised *TnSmu1* circle (*attTnSmu1*; primers B + C). (b) DNA sequence of *attB* and *attTnSmu1*. The predicted 17 bp recombination site is in bold. The 3' end of the leucyl tRNA (*smu_t33*) that overlaps the recombination site is highlighted in gray.

excise (or was below the limit of detection) or that at least one of the primers was either within *TnSmu1* (and not chromosomal DNA) or was too far from the actual recombination sites (*attL* and *attR*). If *TnSmu1* had excised, then the predicted right end is likely not near *smu_209c* or *smu_226c*.

We also designed primers internal to *TnSmu1* but oriented outwards to detect the circularized element (primers B and C in Figure 3a) following excision. PCR with this set of primers would generate a product only if the element excised and both primers are internal to and near the ends of the element. Using genomic DNA as a template (as above), we did not detect a product from PCR using these two primers. This indicates that either *TnSmu1* had not excised (or was below the limit of detection), or that the primers were not internal to and near the ends of the element. If *TnSmu1* had excised, then the predicted right end is likely not near *smu_209c* or *smu_226c*.

We found that this inability to detect excision of *TnSmu1* with the initial primer sets was because *attR* was different from what was postulated initially and not because the element failed to excise. We tested other primer pairs, keeping the primer near *attL* constant and changing the location of the primers near the putative *attR*. We identified PCR primers that produced products that, when sequenced, allowed us to define *attL*, *attR*, *attB*, and *attTnSmu1*

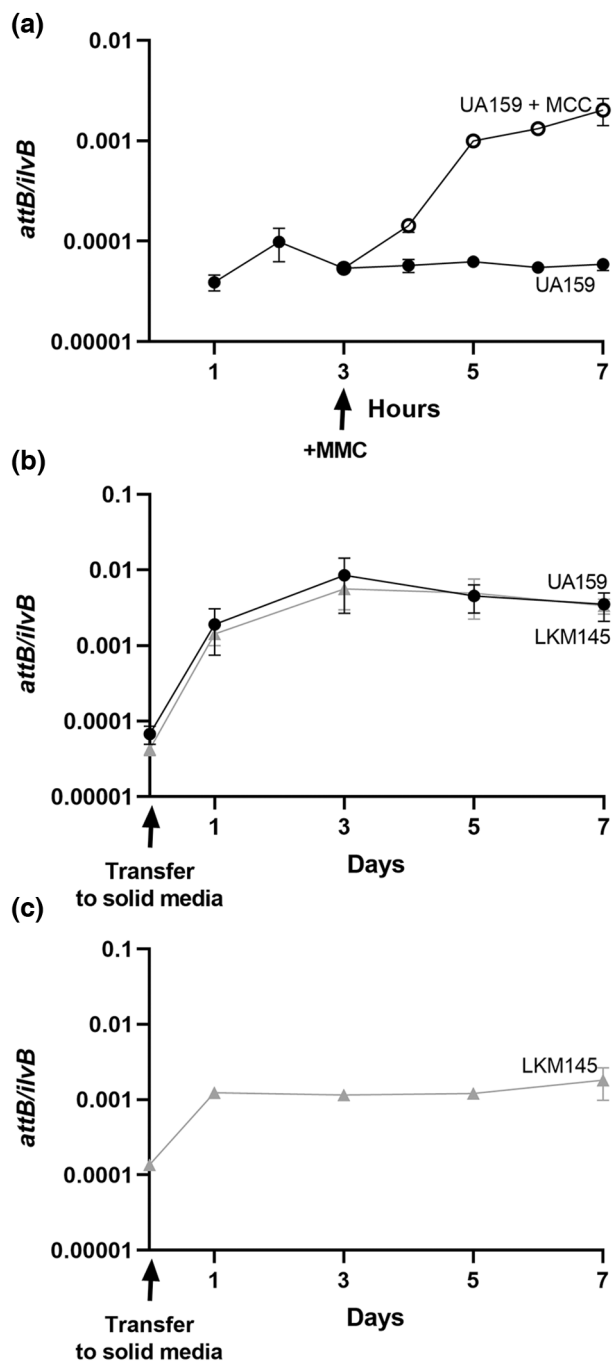


FIGURE 4 Tn*Smu1* excision increases in response to DNA damage and on solid media. Excision of Tn*Smu1* was measured by qPCR to detect *attB* (primers corresponding to A + D indicated in Figure 3). The proportion of cells containing excised Tn*Smu1* was calculated by normalizing *attB* to a nearby chromosomal locus (*ilvB*). Data presented are averages from three or more independent experiments with error bars depicting standard error of the mean. Error bars could not always be depicted due to the size of each data point. (a) *S. mutans* UA159 cells were grown in liquid (TH) medium for 7 h. After 3 h of growth, cells were either left untreated (black circles) or treated with 1 µg/mL mitomycin C (MMC; open circles; time of addition indicated by black arrow below the x-axis). Samples were harvested at the indicated times to measure excision. (b) *S. mutans* strains UA159 (Tn*Smu1*; black circles) and LKM145 (Tn*Smu1*-tet; gray triangles) were grown in TH liquid medium to mid-exponential phase, pelleted, and resuspended at a low density. Cells were then spotted and grown on TH solid medium for 1, 3, 5, or 7 days in anaerobic conditions and samples were taken at the indicated times (days) to measure excision. (c) *S. mutans* strain LKM145 (Tn*Smu1*-tet) was grown in TH liquid medium to mid-exponential phase, pelleted, and resuspended at a low density. Cells were then spotted and grown on BHI solid medium for 1, 3, 5, or 7 days in anaerobic conditions and samples were taken at the indicated times (days) to measure excision.

2.3 | Tn*Smu1* excision increases in response to DNA damage and on solid media

Because Tn*Smu1* has homologs of *immA* and *immR* from ICEBs1 (Figure 2b,c, Table 1) and ICEBs1 is de-repressed by DNA damage, we postulated that DNA damage might also de-repress Tn*Smu1*. Therefore, we measured excision of Tn*Smu1* after addition of mitomycin C (MMC) to cells to induce DNA damage. We purified DNA from cells treated and untreated with MMC and performed qPCR to detect the presence of *attB* (generated upon excision of Tn*Smu1*). We normalized excision to a nearby chromosomal locus (*ilvB*). We found that Tn*Smu1* had excised in ~0.1%–0.2% of cells ($\sim 1\text{--}2 \times 10^{-3}$ *attB*/*ilvB*) after treatment with MMC for 2–4 h. This is ~20–30-fold greater than that in the absence of MMC (~0.006%, $\sim 6 \times 10^{-5}$ *attB*/*ilvB*) (Figure 4a). These results indicate that excision of Tn*Smu1* is induced following DNA damage. We suspect that other conditions that cause DNA damage (e.g., oxidative stress that occurs in the oral cavity) likely cause induction of Tn*Smu1* in a subset of cells.

It also appeared that Tn*Smu1* underwent autonomous replication following excision. Both ICEBs1 and Tn916 undergo autonomous rolling-circle replication following excision (Lee et al., 2010; Wright & Grossman, 2016). This is most easily detected by measuring the relative copy number of the circular element (*attTnSmu1*) to that of the empty chromosomal site (*attB*). Using qPCR to measure *attTnSmu1* and *attB*, we found that during exponential growth, there were approximately 2–5 extrachromosomal copies of Tn*Smu1* per excision event (*attB*), indicating that Tn*Smu1* is capable of autonomous replication, although the copy number was low. By analogy to ICEBs1 and Tn916, Tn*Smu1* most likely undergoes rolling-circle replication that initiates from the origin of transfer (*oriT*) using the element-encoded relaxase (Nick).

(Figure 3). Based on these sites, we conclude that Tn*Smu1* is an approximately 20kb element that extends from open reading frames *smu_191c* through *smu_220c* (Figure 1). The sequences of the various sites also allowed us to identify a 17 bp sequence present in both *attB* and *attTnSmu1* that is likely the recombination site used by the tyrosine recombinase encoded by *int* (*smu_191c*) in Tn*Smu1* (Figure 3b). This is consistent with excision noted by King et al. (2022) when examining read coverage in an *immR*_{*Smu*} mutant. Together, these data demonstrate that Tn*Smu1* is capable of excision from the chromosome of host cells and that a small proportion of cells had “spontaneously” activated Tn*Smu1* in the absence of any exogenous treatment.

As the typical lifecycle of *S. mutans* is within biofilms and on the solid surface of teeth, we sought to determine if TnSmu1 was capable of excision when cells were grown on a solid surface. *S. mutans* cells were grown to mid-exponential phase in TH medium, pelleted, and resuspended at a low cell density. Cells were then spotted onto solid TH medium for 1, 3, 5, or 7 days in anaerobic conditions. We found that over time, excision increased ~10 to 100-fold on solid surfaces compared with liquid culture (Figure 4b).

We also compared wild type *S. mutans* (UA159) with LKM145 (a derivative of UA159 that contains TnSmu1-tet), and found no difference in excision of the element between strains in either liquid or on solid TH media (Figure 4b). We also found that growth in TH liquid medium and plating on BHI solid medium resulted in a similar increase in excision of TnSmu1-tet (Figure 4c), indicating that the change in growth medium did not impact excision.

Together, our results indicate that TnSmu1 is activated when cells are grown on a solid surface, perhaps analogous to the growth in plaque on teeth. This increased activation could also be due to some additional stress experienced during growth on solid surfaces, perhaps resulting in an increase in DNA damage and thus increased activation.

We anticipate that the mechanism of TnSmu1 de-repression is analogous to that for ICEBs1. In the presence of DNA damage-inducing conditions, the ICEBs1-encoded metalloprotease ImmA_{ICEBs1} cleaves the repressor ImmR_{ICEBs1}, thereby causing de-repression of element gene expression (Auchtung et al., 2007; Bose & Grossman, 2011). Based on the similarities between these two ICEBs1 and TnSmu1 regulators, the simplest model is that during DNA damage, ImmA_{smu} becomes activated to cleave and inactivate ImmR_{smu}, thereby causing de-repression of TnSmu1 gene expression. We also note that unlike that for ICEBs1 (Auchtung et al., 2007; Bose & Grossman, 2011), there are no indications that TnSmu1 is regulated by population density, peptide signaling, or quorum sensing as culture density and growth phase did not affect excision frequency (Figure 4a) and there are no genes in TnSmu1 with similarity to known cell-cell signaling systems.

2.4 | TnSmu1 can transfer to *S. mutans* recipients that lack a copy of the element

Based on the presence of an apparently intact set of genes for a T4SS and the ability of TnSmu1 to excise, we tested for the ability of the element to transfer from one cell to another. To monitor transfer of TnSmu1, we constructed *S. mutans* donor and recipient strains that could be distinguished by their unique antibiotic resistances and growth requirements.

2.4.1 | Donors

We introduced a gene conferring tetracycline resistance (*tet*) into TnSmu1 between *smu_210c* and *smu_211c* (Figure 1), generating

TnSmu1-tet (strain LKM145). This insertion is in a region of TnSmu1 with unknown function that we anticipated would not interfere with the typical ICE lifecycle. Indeed, excision of TnSmu1-tet was similar to that of wild type TnSmu1 (Figure 4b).

We also made a mutant of *S. mutans* that requires D-alanine for growth due to a null mutation in *alr* (*alr::erm*), which encodes alanine racemase needed for production of D-alanine (Wecke et al., 1997). Use of an *alr* mutant as a donor allows us to distinguish donors from recipients and transconjugants after the mating because donors will be auxotrophic and unable to grow on media without addition D-alanine. Donors were also defective in genetic competence ($\Delta comS::kan$) (Mashburn-Warren et al., 2010) to prevent transformation with DNA from recipients.

2.4.2 | Recipients

We thought it important to use a recipient that was cured of TnSmu1 (TnSmu1⁰). Some ICEs and temperate phages have immunity and exclusion mechanisms that reduce acquisition of additional copies of the cognate element (Auchtung et al., 2007; Gottesman & Weisberg, 2004; Oppenheim et al., 2005; Serfotis-Mitsa et al., 2008). Notably, ICEBs1 has repressor-mediated immunity (Auchtung et al., 2007). Because TnSmu1 encodes a homolog of ImmR_{ICEBs1}, we were concerned that cells containing TnSmu1 might also have repressor-mediated immunity. Therefore, we used two different recipient strains, one without (denoted $\Delta TnSmu1$ or TnSmu1⁰) and one with TnSmu1 (LMK85 and LMK87, respectively). Of note, we found there was no noticeable growth difference in strains with or without TnSmu1 (Figure S2). Further, both recipients contained a null mutation in *comS* (Mashburn-Warren et al., 2010) to ensure any DNA transfer detected was not via transformation into the recipients.

We found that TnSmu1 transferred from *S. mutans* donors into *S. mutans* recipients provided that the recipients lacked TnSmu1 (Figure 5 and Figure S3). Donors and recipients were grown to mid-exponential phase, pelleted, resuspended at a low cell density, mixed at a ratio of 1:1 and then spotted onto agar plates and allowed to grow for 1, 3, 5, or 7 days. The largest number of TnSmu1 transconjugants was detected 3 days post-inoculation of the mating plates: ~10⁴ transconjugants were detected (Figure 5), corresponding to a mating frequency of ~2 × 10⁻⁵ transconjugants per donor present in the harvested mating mix. The number of transconjugants increased between 1 and 3 days post-inoculation and then dropped at later times (Figure 5). This increase was likely due either to transconjugants dividing and producing progeny or transconjugants becoming donors and further transferring TnSmu1 to additional recipients. The drop in the number of transconjugants detected at later times was most likely due to overall cell death of donors, recipients, and transconjugants that occurred throughout the mating (Figure 5b).

We also measured conjugation efficiencies at different donor to recipient ratios. Transfer was detected at all ratios (1:100, 1:10, 1:1, 10:1, 100:1) and at each of the time points tested (1, 3, 5, 7 days) (Figure S3). The largest number of TnSmu1 transconjugants was

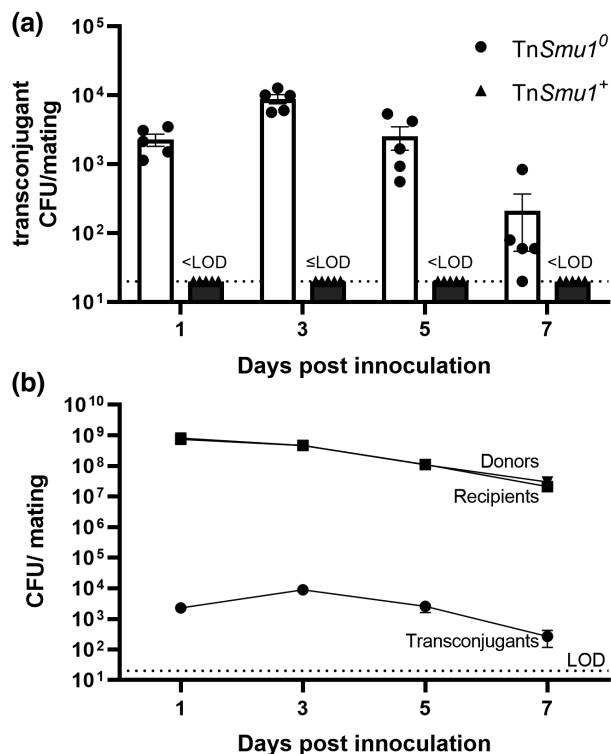


FIGURE 5 TnSmu1 can transfer to recipient cells that lack a copy of the element. Donors containing TnSmu1-*tet* (LKM145) were co-cultured with recipients containing no TnSmu1 (TnSmu1⁰; LKM85) or with TnSmu1 (TnSmu1⁺; LKM87). Cells were grown to mid-exponential phase in TH liquid medium, pelleted and resuspended at a low density, and donors and recipients were mixed at a ratio of 1:1. Mating mixes were spotted onto BHI solid medium and incubated under anaerobic conditions for 1, 3, 5, or 7 days. Cells were then harvested and the numbers of donors (*tet*, *alr*, *kan*), recipients (*alr*+, *spc*), and transconjugants (*tet*, *alr*+, *spc*) were enumerated based on unique phenotypes associated with each cell type. The limit of detection was 20 transconjugant CFUs per mating (1 CFU per plate) as we plated a maximum of one twentieth of the resuspended mating mix. (a) The number of transconjugant CFUs per mating formed with TnSmu1-*tet* donors (LKM145) and TnSmu1⁰ recipients (LKM85, white bars, filled circles are individual data points) or with TnSmu1⁺ recipients (LKM87, dark gray bars, triangles are individual data points). Results with TnSmu1⁺ recipients were at or below the limit of detection (LOD \leq 20 CFU/mating; dotted line). (b) The number of CFUs for donors (inverted triangles), recipients lacking TnSmu1 (squares), and transconjugants (circles) in a mating mix are shown for the experiment in (a). The number of transconjugants increased between 1 and 3 days post inoculation and then dropped. The drop in the number of transconjugants at later times was most likely due to overall cell death that occurred throughout the mating as seen with a parallel drop in numbers of donors and recipients. Data presented are averages from three or more independent experiments. Error bars represent the standard error of the mean and are generally not visible as they are too small relative to the size of each data point. Donor and recipient CFUs are largely indistinguishable in this graph. The dotted line at the bottom represents the limit of detection for all cell types.

detected at 3 days post-inoculation of the mating plates at a donor to recipient ratio of 1:1, and we used these conditions for most experiments.

In contrast to the results with TnSmu1-cured recipients, we detected few, if any, transconjugants in matings with recipients that contained TnSmu1 (Figure 5a and Figure S3). Transconjugants (as detected by tetracycline resistance and growth without D-alanine) were rarely detected, and when they were, we observed only a single colony, indicating that there were \leq 20 total transconjugant CFUs per mating (at or below the limit of detection) at all time points and donor to recipient ratios tested. This represents a decrease of \sim 500-fold compared with isogenic recipients without TnSmu1 (1:1 donors: recipients after 3 days of growth on solid medium). Together, these results show that TnSmu1 is a functional conjugative element, capable of transfer from donor to recipient cells. They also indicate that there is at least one mechanism conferred by TnSmu1 that inhibits acquisition of another copy of the element.

2.5 | Expression of the repressor, ImmR_{Smu}, is sufficient to reduce acquisition of TnSmu1

Because TnSmu1 encodes a homolog of the immunity repressor ImmR from ICEBs1, we postulated that ImmR_{Smu} might also confer some level of immunity that inhibits acquisition of a second copy of the element, analogous to that of ICEBs1 (Auchtung et al., 2007; Bose et al., 2008). Therefore, we sought to determine if expression of the repressor encoded by TnSmu1, in the absence of other TnSmu1 genes, would result in inhibition of (immunity to) acquisition of TnSmu1.

We found that ectopic expression of ImmR_{Smu} in recipient cells inhibited acquisition of TnSmu1. We used recipients that were missing TnSmu1 but expressed *immR*_{Smu} under its predicted endogenous promoter and compared these to recipients with and without TnSmu1, analogous to the experiments described above. We measured acquisition of TnSmu1 after 3 days of mating at a donor to recipient ratio of 1:1. We found that expression of *immR*_{Smu}, in the absence of other genes from the element, reduced acquisition of TnSmu1 to a similar extent (\sim 500-fold) as that of the intact element (Figure 6). Together, these results indicate that expression of the TnSmu1 repressor (ImmR) is sufficient to inhibit acquisition of the element.

2.6 | The preferred integration site of TnSmu1 is in a leucyl-tRNA gene

TnSmu1 resides in donor cells at the 3' end of a leucyl tRNA gene (*smu_t33*) (Figure 3b). We sought to determine if TnSmu1 integrated at this same location following transfer to new cells, that is, in transconjugants, or if it was more promiscuous in site selection, perhaps analogous to Tn916 (Roberts & Mullany, 2009).

We found that following conjugation, TnSmu1 integrated specifically in the 3' end of *smu_t33*. After performing matings into Δ TnSmu1 recipient cells (LKM85) as described above, we isolated 16 independent transconjugants and tested these for integration into

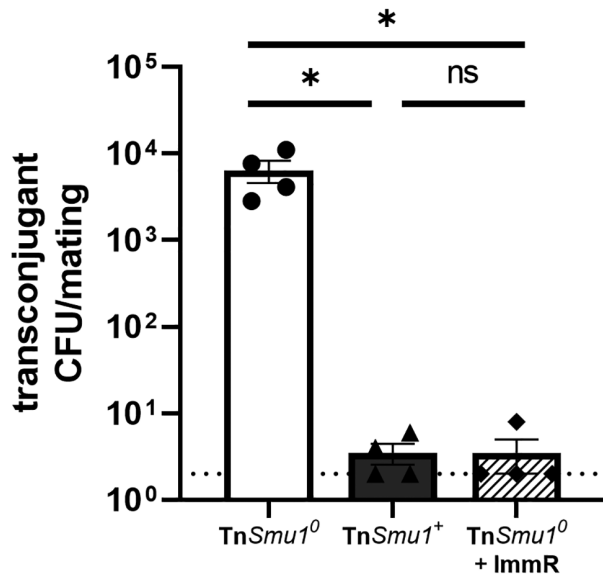


FIGURE 6 Expression of *ImmR_{Smu}* in recipients inhibits acquisition of *TnSmu1*. *TnSmu1-tet* donors (LKM145) were mated with three different recipients: *TnSmu1*⁰ (LKM85, circles, white bar); *TnSmu1*⁺ (LKM87, triangles, dark gray bar); and *TnSmu1*⁰ that expressed *immR_{Smu}* from an ectopic site (LKM233, diamonds, bar with diagonal stripes). Donors and recipients were grown and prepared as described for Figure 5, with donors and recipients mixed at a ratio of 1:1 and transconjugants measured after growth on the solid surface (mating) for 3 days. Data presented are averages from four independent experiments with error bars depicting standard error of the mean. The limit of detection in these experiments was two transconjugant CFUs per mating (up to half of the resuspended mating mix was plated). Results with *TnSmu1*⁺ recipients were at the LOD (2 CFU/mating; dotted line). **p* < 0.05.

smu_t33 using PCR primers that would detect *attL* (Figure 3a; Section 2). We found that *TnSmu1* had integrated into *smu_t33* in all 16 of the transconjugants tested. This tRNA gene (*smu_t33*) and the 17bp *attB* are not found anywhere else in the *S. mutans* genome (Ajdic et al., 2002). Together, our results indicate that the identified 17bp site referred to as *attB* (Figure 3b) is the preferred site of integration of *TnSmu1*. That said, we cannot rule out the possibility that *TnSmu1* might integrate into other sites in the chromosome at a low frequency.

2.7 | *TnSmu1* causes a growth arrest in host cells

Tn916, an ICE related to *TnSmu1*, causes growth arrest and death of host cells following excision and expression of its genes (Bean, McLellan, & Grossman, 2022b). In contrast, ICEBs1, which encodes a T4SS and regulatory proteins similar to those encoded by *TnSmu1*, does not cause death of its host cells (Babic et al., 2011; Bean, McLellan, & Grossman, 2022b). Therefore, we wondered whether or not *TnSmu1* manipulated the growth and or viability of its host cells. As *TnSmu1* only excises in a relatively small fraction of cells (Figure 4), we decided to examine *TnSmu1* activation in single cells using fluorescence microscopy and a fluorescent reporter that would be indicative

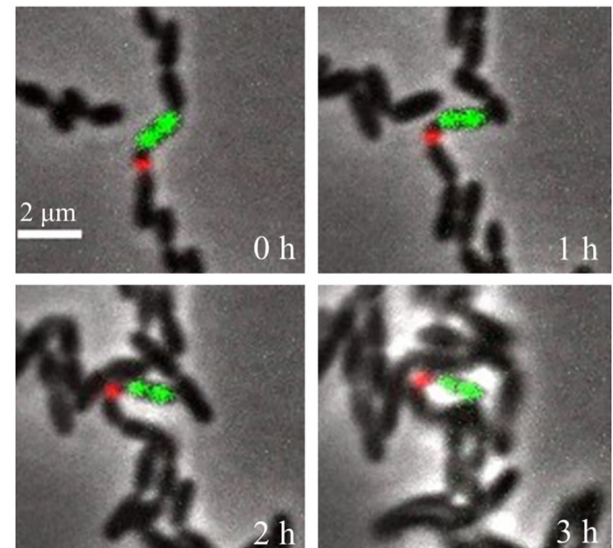


FIGURE 7 Cells with an active *TnSmu1* stop growing. Cells containing *TnSmu1-gfp-tet* (LKM137) were grown in TH liquid medium to late exponential phase. At time 0 h, cells were spotted onto agarose pads containing TH medium, 0.1 M propidium iodide, and 0.35 μg/mL DAPI. Cells were monitored by phase contrast and fluorescence microscopy for 3 h. GFP (green) was produced in cells in which *TnSmu1* was activated and excised from the chromosome. Propidium iodide (red) indicates cell death. Images shown are a merge of phase contrast and fluorescence. Three independent experiments gave similar results and were quantified (described in results), in total analyzing 82 cells from ~30 individual microscope frames. Of the 82 cells observed with an active *TnSmu1-GFP* (GFP on, green), 94% (77/82) did not undergo any further cell divisions, and 6% (5/82) divided once. Of 82 neighboring cells that had not activated *TnSmu1-GFP* (GFP off), only 4% (3/82) of cells did not undergo any further cell divisions, and 96% (79/82) of cells underwent one or more cell divisions. A representative set of images is shown here. DAPI is not shown for visual clarity.

of *TnSmu1* gene expression. We inserted *gfpmut2* between *smu_210* and *smu_211* in *TnSmu1* (Figure 1) to generate *TnSmu1-gfp* (LKM137). Cells should fluoresce green only when *TnSmu1* genes are expressed. Insertion of *gfp* within *TnSmu1* did not have a significant impact on excision: the frequency of excision of *TnSmu1-gfp* (~0.004%, ~4x10⁻⁵ *attB*/*ilvB*) during growth in liquid medium was similar to that of wild type *TnSmu1* and *TnSmu1-tet* (Figure 4b).

We found that cells expressing *TnSmu1-gfp* had a growth defect. Cells containing *TnSmu1-gfp* were diluted to early exponential phase, grown for 3 h, and then spotted onto an agarose pad on a microscope slide. Cells were visualized and tracked for 3 h, comparing those that had activated *TnSmu1-gfp* to those that had not. We tracked 82 cells in which *TnSmu1-gfp* was activated (GFP on) and 82 neighboring cells in which *TnSmu1-gfp* was apparently not activated (GFP off) (Figure 7). Of the cells activating *TnSmu1* (GFP on), 94% (77/82) did not undergo any further cell divisions and 6% (5/82) divided once (Figure 7). In contrast, in the 82 neighboring cells without *TnSmu1-GFP* activated (GFP off), only 4% (3/82) of cells did not undergo any further cell divisions, and 96% of cells underwent 1 or more cell divisions (79/82) (77/82 vs. 3/82, $\chi^2 = 133.64$, *p* < 0.0001).

Although the cells expressing TnSmu1 had a growth arrest, we found no evidence of cell death. Using propidium iodide (PI) to monitor cell viability, we found that of the 82 cells that had activated TnSmu1-GFP, only 12% (10/82) became or had progeny that became PI-positive during the course of the experiment (Figure 7). This was not significantly different from that of cells without TnSmu1 activated: 13% of cells became PI-positive or had progeny that became PI-positive (11/82) throughout the experiment. These numbers are consistent with *S. mutans* viability of randomly selected wild type cells (UA159, 10/82) and cells without TnSmu1 (LKM68, 9/82). This is also consistent with what is seen in *S. mutans* biofilms and various growth conditions via fluorescence microscopy (Decker, 2001; Decker et al., 2014; Zhang et al., 2009). Together, these results indicate that cells in which TnSmu1 becomes activated are unable to divide; however, they do not lose viability, at least over a period of 3 h.

3 | DISCUSSION

Our work demonstrates that TnSmu1 is a functional ICE, capable of excision from the host cell chromosome and transfer to recipient cells. We found that activation of TnSmu1 is stimulated by DNA damage and by growth on a solid surface. Further, activation of TnSmu1 caused a growth arrest, indicating that it can have a profound effect on host physiology. Our findings provide a basis for future work examining the impacts of TnSmu1 on the physiology of *S. mutans*. Further, as ICEs can be utilized for genetic engineering purposes (Bean, Herman, et al., 2022a; Brophy et al., 2018; Miyazaki & van der Meer, 2013; Peters et al., 2019), TnSmu1 may perhaps be developed as an engineering tool for manipulation of organisms in the oral microbiome.

3.1 | The TnSmu1 repressor

immR_{Smu} (*smu_218c*) almost certainly encodes the repressor of TnSmu1, based on three lines of evidence. First, *ImmR_{Smu}* is similar to the repressor of ICEBs1 and others in this family. Second, like other 'immunity' repressors, expression in recipient cells (in the absence of other element genes) caused a reduction in acquisition of a copy of the element, similar to immunity to superinfection exhibited by various temperate phages (Gottesman & Weisberg, 2004; Oppenheim et al., 2005) and ICEBs1 (Auchtung et al., 2007; Bose et al., 2008). Lastly, *smu_218c* (*immR*) appears to be an essential gene based on Tn-seq experiments with *S. mutans* (Shields et al., 2018). Repressors of mobile genetic elements that integrate and excise (e.g., ICEs and temperate phages) can appear to be 'essential' because their loss can result in excision and loss of the element in which they are encoded. For example, if loss of a repressor leads to excision of the element, that element will likely be lost from the population of cells. This loss makes it very difficult to establish a null mutation in the gene for the repressor as the loss of function mutation in the repressor gene will be lost along with the resulting excised element. In this way, genes potentially encoding element repressors can be identified in

genome-wide screens and appear as "essential" even though they reside in an element that itself is not essential. This point is highlighted by the fact that we were able to delete TnSmu1 and cells are viable, but the repressor appears to be essential (Shields et al., 2018).

3.2 | Costs and benefits to cells carrying an ICE

ICEs are often double-edged swords to their host cells: They can provide both fitness costs and benefits. They can benefit their host cells through associated cargo genes that confer specific phenotypes, such as antibiotic resistances, metabolic traits, and virulence factors. However, some ICEs can manipulate host development, growth, and viability (Beaber et al., 2004; Bean, McLellan, & Grossman, 2022b; Jones et al., 2021; Pembroke & Stevens, 1984; Reinhard et al., 2013). This is similar to plasmids, which are known to provide beneficial phenotypes to their hosts but are energetically costly to maintain (San Millan & MacLean, 2017).

This complex interplay between element and host is evident in Tn916 and *Pseudomonas* ICE_{clc}. Tn916 was discovered through its ability to spread tetracycline resistance through clinical isolates of *Enterococcus* (Franke & Clewell, 1981a, 1981b), thus providing a clear benefit to its host cells. However, activation of Tn916 halts cell growth and leads to decreased bacterial viability (Bean, McLellan, & Grossman, 2022b). Similarly, when activated, ICE_{clc} causes slow growth and decreased viability (Reinhard et al., 2013). These growth defective cells are in a "transfer competent state." Deletion of the genes required for the decreased cell growth and viability cause a decrease in conjugation efficiency. This indicates that this state of decreased cell growth and viability is important for efficient transfer of ICE_{clc} (Delavat et al., 2016; Reinhard et al., 2013).

There are certainly parallels between the growth arrest caused by TnSmu1, Tn916, and ICE_{clc}. However, unlike Tn916 and ICE_{clc}, our results indicate that TnSmu1 does not cause host cell death. Additionally, a CRISPRi knockdown of *immR_{Smu}* caused an arrest in growth of the entire population (King et al., 2022). It is possible that the cells with an activated TnSmu1 die following growth arrest, but we have not observed this, nor have assays measuring death been reported. The apparent essentiality of *immR_{Smu}* (Shields et al., 2018) could indicate that there is cell death following inactivation of the repressor and subsequent activation of TnSmu1. However, as discussed above, we postulate that this apparent essentiality is due to excision and loss of TnSmu1 and the consequent loss of the *immR* null allele in TnSmu1. This further begs the questions: What is the mechanism of the growth arrest caused by activation of TnSmu1, is this growth arrest important for conjugation and transfer, and is there a benefit that TnSmu1 confers to host cells?

3.3 | Host range of TnSmu1

Bioinformatic searches indicate that TnSmu1 is naturally located within *S. mutans* species. However, it is not known if TnSmu1 is

capable of transfer to other bacterial species typically found in the oral cavity. For many ICEs, there is a difference between naturally occurring host range and experimental host range. For example, ICEBs1 is naturally found only in *Bacillus* sp. but can transfer to a diverse array of other microbes (Auchtung et al., 2005; Brophy et al., 2018). Tn916 is naturally found in *Enterococcus*, *Clostridium*, *Streptococcus*, and *Staphylococcus* species. However, it is also functional in *Bacillus* sp. [e.g., (Roberts & Mullany, 2009, 2011; Wright & Grossman, 2016)]. Understanding experimental host range allows utilization of ICEs for genetic engineering purposes to a wider diversity of organisms. Further, many ICEs are able to mediate transfer of other mobile genetic elements, including plasmids that replicate by rolling-circle replication (Johnson & Grossman, 2015; Lee et al., 2012; Santoro et al., 2014). We suspect that Tn*Smu1* is able to drive transfer of plasmids and other mobile genetic elements found within the oral microbiome. As many mobile genetic elements encode antibiotic resistance, the impact of Tn*Smu1* on clinically important phenotypes (virulence traits and drug resistances) may extend beyond transfer of Tn*Smu1* alone.

4 | MATERIALS & METHODS

4.1 | Media and growth conditions

For liquid growth, *S. mutans* cultures were grown statically in 50% Todd Hewitt (TH) broth in tightly closed 15ml conical tubes. For growth on solid media, *S. mutans* were grown on Brain Heart Infusion (BHI) plates (or TH plates where indicated) with 1.5% agar under anaerobic conditions (using Anaerogen Anaerobic Gas Generator, Hardy Diagnostics). Cultures and plates were incubated at 37°C. When appropriate, media were supplemented with 1.6 mg/mL D-alanine. Antibiotics were used at the following concentrations: 1 mg/mL kanamycin, 1 mg/mL spectinomycin, 10 µg/mL erythromycin.

4.2 | Strains and alleles

S. mutans strains (Table 2) were derived from *S. mutans* UA159 (ATCC 700610) (Ajdic et al., 2002) and were made by natural transformation (Li et al., 2001; Petersen & Scheie, 2010). New alleles were constructed as double crossover events using long-flanking homology PCR by isothermal assembly (Gibson et al., 2009; Xie et al., 2011). Markers used to select for transformants were *spc* (spectinomycin resistance), *erm* (erythromycin resistance), *tet* (tetracycline resistance), or *kan* (kanamycin resistance). All mutants were constructed in a clean, isogenic background and alleles were confirmed through Sanger sequencing. Any alleles obtained from other sources were moved into a clean, isogenic background. Construction of new strains and alleles is summarized below.

ΔTn*Smu1::spc* (constructed in LKM68 then transferred via natural transformation to LKM85 and LKM233) was constructed by

replacing Tn*Smu1* with the spectinomycin resistance cassette from pUS19 (Benson & Haldenwang, 1993). The *attL* recombination site within *smu_t33* was left intact (leaving 4 bp downstream of the 3' end of *smu_t33*, thus leaving intact the tRNA gene *smu_t33*), but the *attR* recombination site was removed (preserving 67bp downstream of the 3' end of *smu_221c*). The allele was constructed via isothermal assembly of the antibiotic resistance cassette and ~750bp of upstream and downstream homology arms.

ΔTn*Smu1::kan* (constructed in LKM139 then transferred via natural transformation to LKM167) was made in the same way as ΔTn*Smu1::spc*, with the same borders, except that the kanamycin resistance cassette from pGK67 (Lemon et al., 2001) was used instead of *spc*.

Δ(*smu_t33*-Tn*Smu1*)::*kan* in LKM141 deletes Tn*Smu1* and the tRNA gene *smu_t33* and inserts *kan* from pGK67. The deletion endpoints extend from 14bp downstream of *smu_t32* through *attR*, leaving *smu_221c* (the gene downstream of Tn*Smu1*) intact, and ending 67bp downstream from the *smu_221c* stop codon. The allele was constructed via isothermal assembly of the antibiotic resistance cassette and ~750bp of upstream and downstream homology arms. Although *smu_t33* encodes a unique tRNA, it was not essential: the deletion was viable, albeit with a growth defect.

Δ*agaL::spc* (constructed in LKM62 and then transferred via natural transformation to LKM87) was constructed by replacing the *agaL* open reading frame (maintaining the first 558bp and last 458bp of the *agaL* open reading frame) with the spectinomycin resistance cassette from pUS19. The allele was constructed via isothermal assembly of the antibiotic resistance cassette and ~750bp of upstream and downstream homology arms. *agaL* is considered a non-essential chromosomal location suitable for cloning (Reck & Wagner-Döbler, 2016).

Tn*Smu1-tet* (initially in LKM76 and then transferred via natural transformation to make LKM145) was constructed by inserting the tetracycline resistance cassette (*tetM*) 3 bp downstream of the 3' end of *smu_211c*. The allele was constructed via isothermal assembly of the antibiotic resistance cassette and ~750bp of upstream and downstream homology arms. *tetM* from Tn916 was used to confer tetracycline resistance from CMJ253 (including 376bp upstream of *tetM* so as to include the *tetM* promoter) (Johnson & Grossman, 2014). *tetM* was co-directional with the upstream and downstream genes in Tn*Smu1* and did not contain a transcriptional terminator downstream of *tetM*. Tn*Smu1 gfpmut2-tet* in LKM137 was constructed in an identical manner by inserting *gfpmut2* allele and *tetM* from Tn916 from CMJ253 (Johnson & Grossman, 2014) 3 bp downstream of the 3' end of *smu_211c*. *gfpmut2* was obtained from ELC1458 (Bean, McLellan, & Grossman, 2022b). *gfpmut2* is promoter-less and co-directional with the upstream and downstream genes in Tn*Smu1*. It has the *B. subtilis spoVG* ribosome-binding site to initiate translation.

Δ*alr::erm* (initially in LKM127 and then transferred via natural transformation to make LKM145) was constructed via isothermal assembly of the erythromycin antibiotic resistance cassette (*erm*) and ~750bp of upstream and downstream homology arms. The first 4 bp of the *alr* open reading frame was retained as it overlapped

TABLE 2 *S. mutans* strains

Strain ¹	Relevant genotype (reference; comment)
UA159	Originally isolated from a child with active caries, GenBank: AE014133.2 (Ajdic et al., 2002)
LKM62	Δ agaL::spc (used to construct LKM87)
LKM68	Δ TnSmu1::spc ² (used to construct LKM85, LKM167, LKM233, used to determine growth of Δ TnSmu1 compared to WT UA159)
LKM69	Δ comS::kan (used to construct LKM145)
LKM76	TnSmu1-tet ³ (used to construct LKM145)
LKM85	Δ TnSmu1::spc ² Δ comS::erm ⁴ (used as recipient in matings)
LKM87	Δ agaL::spc Δ comS::erm ⁴ (used as recipient in matings, Δ agaL::spc was used as a selectable marker to confirm identify of transconjugants)
LKM127	Δ alr::erm (used to construct LKM145, Δ alr::erm was used to provide counterselection to prevent donor growth)
LKM137	TnSmu1-(gfpmut2 tet) ⁵ (insertion downstream from gene smu_211c, used to monitor cells with TnSmu1 expression)
LKM139	Δ TnSmu1::kan ² (used to construct LKM167); leaves smu_t33 (tRNA) intact
LKM141	Δ (smu_t33-TnSmu1)::kan ⁶ (used to determine essentiality of smu_t33)
LKM145	TnSmu1-tet ³ Δ alr::erm Δ comS::kan (used as donor during mating assays, Δ alr::erm was used to provide counterselection to prevent donor growth)
LKM164	Δ lacE::(attB _{Smu} spc) ⁷ (used to construct LKM167)
LKM165	Δ lacE::(attTnSmu1 spc) ⁸ (used as qPCR standard curve control)
LKM167	Δ lacE::(attB _{Smu} spc) ⁷ Δ TnSmu1::kan ² (used as qPCR standard curve control)
LKM218	Δ agaL::(immR _{Smu} kan) ⁹ (used to construct LKM233)
LKM233	Δ TnSmu1::spc ² Δ agaL::(immR _{Smu} kan) ⁹ Δ comS::erm ⁴

¹Strains are derived from UA159.

² Δ TnSmu1::spc was constructed by replacing TnSmu1 with the spectinomycin resistance cassette. The attL recombination site within smu_t33 was left intact but the attR recombination site was removed. Δ TnSmu1::kan was constructed in an identical fashion instead using the kanamycin resistance cassette.

³TnSmu1-tet contains the tetracycline resistance cassette tetM inserted 3 bp downstream of the 3' end of smu_211c.

⁴ Δ comS::erm was kindly provided by Stephen J. Hagen (Son et al., 2012).

⁵TnSmu1-(gfpmut2 tet) contains gfpmut2 and tetM 3 bp downstream of the 3' end of smu_211c.

⁶ Δ (smu_t33-TnSmu1)::kan replaces smu_t33 and TnSmu1 with the kanamycin resistance cassette. The TnSmu1 attL/attR recombination sites were also deleted and the tRNA gene smu_t33 is disrupted. These cells are viable, so this gene is not essential.

⁷ Δ lacE::(attB_{Smu} spc) contains the genomic attachment site for TnSmu1 cloned, along with a spectinomycin resistance cassette, into lacE.

⁸ Δ lacE::(attTnSmu1 spc) contains the attachment site from the TnSmu1 circle cloned, along with a spectinomycin resistance cassette, into lacE.

⁹ Δ agaL::(immR_{Smu} kan) contains immR_{Smu} (including the putative promoter) and kan cloned into agaL.

with *acpS*, but the rest of the *alr* open reading frame was deleted (to 172 bp upstream of the 5' end of *recG*). The erythromycin resistance cassette from pCAL215 was used (Auchtung et al., 2007), originally derived from pDG795 (Guérout-Fleury et al., 1996).

Δ comS::kan (originally in LKM69 and then transferred via natural transformation to make LKM145) was constructed by replacing the entire *comS* open reading frame with the kanamycin resistance cassette from pGK67. The allele was constructed via isothermal assembly of the antibiotic resistance cassette and ~750 bp of upstream and downstream homology arms. The Δ comS::erm allele was kindly provided by Stephen J. Hagen and construction was previously described (Son et al., 2012). This allele was transferred via natural transformation to LKM85, LKM87, and LKM233.

Δ agaL::(immR_{Smu} kan) (*smu_218c* kan) (initially in LKM218 and then transferred via natural transformation to make LKM233) was constructed by replacing the *agaL* open reading frame with immR_{Smu}

and kan (maintaining the first 558 bp and last 458 bp of the 2,160 bp *agaL* open reading frame). immR_{Smu} was cloned in the opposite orientation of *agaL* to prevent expression from the *agaL* promoter. immR_{Smu} was amplified from TnSmu1 from *S. mutans* UA159, amplifying 746 bp upstream of the 5' end of immR_{Smu} such that it contains the predicted promoter driving expression of immR_{Smu}, through the end of the immR_{Smu} open reading frame. The *gatB/yerO* bidirectional terminator from *B. subtilis* was added 6 bp downstream of the stop codon of immR_{Smu} to prevent possible transcriptional conflict from the *agaL* promoter. The organization of TnSmu1 is reminiscent of that of ICEBs1 where immR and immA are co-transcribed and divergent from most of the genes in the element (Auchtung et al., 2007; Bose et al., 2008). Therefore, we predicted the intergenic region between *smu_217c* and immR_{Smu} (*smu_218c*) would contain the promoter of ImmR_{Smu}. The kanamycin resistance cassette from pGK67 was cloned divergent to immR_{Smu}. The allele was constructed via

isothermal assembly of the antibiotic resistance cassette, the *imR_{Smu}* fragment, and ~750bp of upstream and downstream homology arms. *agaL* is a non-essential chromosomal location suitable for cloning (Reck & Wagner-Döbler, 2016).

$\Delta lacE::(attTnSmu1\ spc)$ in LKM165 was constructed by inserting *attTnSmu1* and *spc* into *lacE*, maintaining the first 512bp and the last 463bp of the *lacE* open reading frame. *attTnSmu1* and the surrounding regions in *TnSmu1* (containing the last 730bp of the *int_{Smu}* open reading frame and the first 157bp of the *smu₂₂₀* open reading frame) were amplified from *TnSmu1* that had been spontaneously excised from liquid cultures of *S. mutans* UA159. The spectinomycin resistance cassette from pUS19 was used. The allele was constructed via isothermal assembly of the antibiotic resistance cassette, the *attTnSmu1* fragment, and ~750bp of upstream and downstream homology arms. *lacE* is considered a non-essential chromosomal location suitable for cloning (Reck & Wagner-Döbler, 2016).

$\Delta lacE::(attB_{Smu}\ spc)$ (initially in LKM164 and then transferred via natural transformation to make LKM167) was constructed by inserting *attB_{Smu}* and *spc* into *lacE* (with regions of *lacE* as described above). *attB_{Smu}* was constructed by amplifying the genomic region upstream of *attL* (including the last 16bp of *smu_{t24}* to 5 bp downstream of the 3' end of *smu_{t33}* so that the recombination site *attB* is present) and stitching it together with the genomic region downstream of *attR* (from 67bp downstream of the 3' end of *smu₂₂₁* to 124bp upstream of the 5' end of *smu₂₂₁*) and cloned into pCAL1422 (Thomas et al., 2013). The *attB_{Smu}* was amplified from the resulting plasmid and the spectinomycin resistance cassette was amplified from pUS19. The allele was constructed via isothermal assembly of the antibiotic resistance cassette, the *attB_{Smu}* fragment, and ~750bp of upstream and downstream homology arms.

4.3 | Homology, bioinformatic analyses, and *TnSmu1* conservation

Global alignments between *TnSmu1* were calculated with EMBOSS Needle pairwise global sequence alignment (Needleman & Wunsch, 1970). BLASTp and BLASTn publicly available databases were accessed on June 9, 2022. Structural predictions were done using Phyre2, accessed June 9, 2022. Helix-turn-helix domains were predicted using GYM 2.0 (Narasimhan et al., 2002).

We used cblaster (Gilchrist et al., 2021) to look at conservation of *TnSmu1* across sequences of *S. mutans* publicly available as of June 22, 2022. We used the predicted protein sequences of the genes within *TnSmu1* as the query for cblaster. Subjects were grouped into clusters based on BLASTp hits to *TnSmu1* protein sequence and ranked by cluster similarity. Cluster similarity score is calculated by cblaster as $S = h + i \cdot s$, where h is the number of query sequences with BLASTp hits, s is the number of contiguous gene pairs with conserved synteny, and i is a weighting factor (default value 0.5) determining the weight of synteny in the similarity score. If a *S. mutans* strain appeared twice due to multiple copies of the genome

sequence available in the NCBI database, the genome with the lower cluster similarity score was excluded from Figure S1.

4.4 | Determination of *TnSmu1* excision and integration

Genomic DNA was isolated from overnight cultures of *S. mutans* UA159 using Qiagen DNeasy kit with 40mg/mL lysozyme. *TnSmu1* excision and the resulting *attB* sequence was identified with primers oLM27 (5'-ACACCAGATTGTGCTCTG) and oLM49 (5'-GGCAAGTCTTGATTATCGCTTTAGAAAGAG). The *attTnSmu1* junction formed via site-specific recombination was determined using primers oLM38 (5'-CATCAAGTTAGCACAGTCAGATAAAATCG) and oLM107 (5'-CATAATAGGTTCCATTAACTACTGCC). The resulting products were determined by Sanger sequencing. The location of integrated *TnSmu1* in transconjugants was confirmed using primers oLM40 (5' - CGACCAAAGAAAAATTATCTCAAGAGACAAAG -3') and oLM44 (5'-GGCAGACGCGCTGGAC -3') that detected *attL* within *smu_{t33}*.

4.5 | Quantitative PCR to determine excision and replication of the element

Overnight cultures were diluted to OD = 0.05 in 50% TH medium and grown at 37°C. After 3 h of growth, the culture was split and 1 µg/mL Mitomycin C (MMC) was added to half of the culture (where indicated). Samples were taken every hour pre- and post-MMC addition and into stationary phase (7 h total). Genomic DNA was isolated using Qiagen DNeasy kit. Excision was measured using primers oLM166 (5'-TTGGTTCGAATCCAGCTACC) and oLM109 (5'-GACTTATGGTCATTGTTGCG) to amplify the vacant insertion site *attB*. *attB* amplification was normalized to a control chromosomal region in *ilvB*, which is ~7 kb downstream of *attB*. *ilvB* was amplified with primers oLM173 (5'-AGGTGGCGGTGTCAATTATG) and oLM174 (5'-GCATCTCCCACTGGAATAG). The copy number of the *TnSmu1* circle was measured with primer pair oLM224 (5'-AATCTTCTATCCCAATTTCTCCC) and oLM226 (5'-TGGGAGAAATTTGGGAGAGAAAATC) to quantitate the unique *attTnSmu1* junction formed via site-specific recombination. To determine if *TnSmu1* was replicating, we determined the ratio of the number of copies of circular *TnSmu1* (*attTnSmu1*) to the number of copies of the excision site (*attB*).

qPCR was done using SSoAdvanced SYBR master mix and CFX96 Touch Real-Time PCR system (Bio-Rad). Copy numbers of *attP* and *attB* were determined by the Pfaffl method (Pfaffl, 2001). Standard curves for *attTnSmu1*, *attB*, and the control chromosome locus *ilvB* were generated from genomic DNA of LKM165, LKM167, and *S. mutans* UA159, respectively. LKM165 contains an ectopic copy of *attTnSmu1* inserted at *lacE*. LKM167 does not contain *TnSmu1* and therefore contains a copy of the unoccupied chromosome site *attB*.

inserted at *lacE*. *S. mutans* UA159 was considered the wild type and was used for measuring the nearby chromosomal locus, *ilvB*.

4.6 | Growth curves

Strains were grown in 50% TH broth overnight. Cultures were diluted to an OD₆₀₀ of 0.05 and grown statically in closed 15 ml conical tubes. The number of colony forming units (CFUs) and OD₆₀₀ was determined every hour. Cells were monitored for 7 h of growth.

4.7 | Mating assays

Donor and recipient cells were diluted to early exponential phase and grown to mid-exponential phase over 4 h. Cells were then pelleted at 5000rpm for 5 mins and resuspended to an OD of 0.01 in 1x Spizizen's salts (Harwood & Cutting, 1990). Donor and recipient cells were combined at various ratios and 50 µl of each mix was spotted onto a BHI plate (or TH plate) supplemented with D-alanine. Mating plates were then incubated at 37°C in anaerobic conditions (using Anaerogen Anaerobic Gas Generator, Hardy Diagnostics) for up to 7 days. Spots were then harvested by scrapping the spot into 1x Spizizen's salts and vortexed. Cells were then plated on selective media to detect *TnSmu1* transfer. The number of donor (tetracycline-resistant, D-alanine auxotrophs), recipient (tetracycline sensitive, D-alanine prototrophs), and transconjugant (tetracycline-resistant, D-alanine prototrophs) CFUs were enumerated both pre- and post-mating. Conjugation efficiency was calculated as the percentage of transconjugant CFUs formed normalized to the number of donor cells harvested at the end of the mating to account for cell growth.

4.8 | Time-lapse microscopy and analysis

S. mutans cells were diluted to early exponential phase in 50% TH media. After 3 h of growth to late exponential phase, cells were transferred to an agarose pad (1.5% UltraPure agarose, Invitrogen; dissolved in growth medium) containing 0.1 M propidium iodide and 0.35 µg/mL DAPI. The agarose pad was created in an incubation chamber, which was made by stacking two Frame-Seal Slide Chambers (Bio-Rad) on a standard microscope slide (VWR). Cells were then grown at 37°C for 3 h while monitoring growth. Fluorescence was generated using a Nikon Intensilight mercury illuminator through appropriate sets of excitation and emission filters (Chroma; filter sets 49,000, 49,002, and 49,008). Time-lapse images were captured on a Nikon Ti-E inverted microscope using a CoolSnap HQ camera (Photometrics). ImageJ software (Schindelin et al., 2012) was used for image processing and analysis.

AUTHOR CONTRIBUTIONS

Lisa K. McLellan: Conceptualized, investigated, validated, visualized, wrote (original and editing); **Mary E. Anderson:** Investigated,

validated, visualized, wrote (editing); **Alan D. Grossman:** Conceptualized, funding acquisition, supervision, wrote (original manuscript and editing).

ACKNOWLEDGMENTS

We thank Katharina Ribbeck (MIT, Cambridge, MA), Dan Smith (Forsyth Institute, Cambridge, MA) for sharing strains. We thank Stephen J. Hagen (University of Florida, Gainesville, FL) for kindly sharing strains and the $\Delta comS::erm$ allele, James S. Weagley (Washington University, St. Louis, MO) for thoughtful conversations on bioinformatic analyses of *TnSmu1* distribution among bacterial species and Sang-Joon Ahn (University of Florida, Gainesville, FL) for useful conversations and Robert Shields (Arkansas State University) for discussions regarding results and appropriate nomenclature for genes in *TnSmu1*. Research reported here is based upon work supported, in part, by the National Institute of General Medical Sciences of the National Institutes of Health under award number R35 GM122538 to ADG. Any opinions, findings, and conclusions or recommendations expressed in this report are those of the authors and do not necessarily reflect the views of the National Institutes of Health.

CONFLICT OF INTEREST

The authors have declared that no competing interests exist.

DATA AVAILABILITY STATEMENT

The data that support the findings of this study are available from the corresponding author upon reasonable request.

ETHICS STATEMENT

No human or animal subjects were used in this study.

ORCID

Lisa K. McLellan  <https://orcid.org/0000-0001-6418-8039>

Mary E. Anderson  <https://orcid.org/0000-0002-6930-3830>

Alan D. Grossman  <https://orcid.org/0000-0002-8235-7227>

REFERENCES

- Ajdic, D., McShan, W.M., McLaughlin, R.E., Savic, G., Chang, J., Carson, M.B. et al. (2002) Genome sequence of *Streptococcus mutans* UA159, a cariogenic dental pathogen. *Proceedings of the National Academy of Sciences of the United States of America*, 99, 14434–14439.
- Alvarez-Martinez, C.E. & Christie, P.J. (2009) Biological diversity of prokaryotic type IV secretion systems. *Microbiology and Molecular Biology Reviews*, 73, 775–808.
- Auchtung, J.M., Lee, C.A., Monson, R.E., Lehman, A.P. & Grossman, A.D. (2005) Regulation of a *Bacillus subtilis* mobile genetic element by intercellular signaling and the global DNA damage response. *Proceedings of the National Academy of Sciences of the United States of America*, 102, 12554–12559.
- Auchtung, J.M., Lee, C.A., Garrison, K.L. & Grossman, A.D. (2007) Identification and characterization of the immunity repressor (ImmR) that controls the mobile genetic element ICEBs1 of *Bacillus subtilis*. *Molecular Microbiology*, 64, 1515–1528.
- Auchtung, J.M., Aleksanyan, N., Bulku, A. & Berkmen, M.B. (2016) Biology of ICE Bs1, an integrative and conjugative element in *Bacillus subtilis*. *Plasmid*, 86, 14–25.

- Babic, A., Berkmen, M.B., Lee, C.A. & Grossman, A.D. (2011) Efficient gene transfer in bacterial cell chains. *mBio*, 2, e00027-11.
- Beaber, J.W., Hochhut, B. & Waldor, M.K. (2004) SOS response promotes horizontal dissemination of antibiotic resistance genes. *Nature*, 427, 72–74.
- Bean, E.L., Herman, C., Anderson, M.E. & Grossman, A.D. (2022a) Biology and engineering of integrative and conjugative elements: construction and analyses of hybrid ICEs reveal element functions that affect species-specific efficiencies. *PLoS Genetics*, 18, e1009998.
- Bean, E.L., McLellan, L.K. & Grossman, A.D. (2022b) Activation of the integrative and conjugative element Tn916 causes growth arrest and death of host bacteria. *PLoS Genetics*, 18, e1010467.
- Benson, A.K. & Haldenwang, W.G. (1993) Regulation of sigmaB levels and activity in *Bacillus subtilis*. *Journal of Bacteriology*, 175, 2347–2356.
- Berkmen, M.B., Lee, C.A., Loveday, E.-K. & Grossman, A.D. (2010) Polar positioning of a conjugation protein from the integrative and conjugative element ICEBs1 of *Bacillus subtilis*. *Journal of Bacteriology*, 192, 38–45.
- Bhatty, M., Laverde Gomez, J.A. & Christie, P.J. (2013) The expanding bacterial type IV secretion lexicon. *Research in Microbiology*, 164, 620–639.
- Bi, D., Xu, Z., Harrison, E.M., Tai, C., Wei, Y., He, X. et al. (2012) ICEberg: a web-based resource for integrative and conjugative elements found in bacteria. *Nucleic Acids Research*, 40, D621–D626.
- Bose, B. & Grossman, A.D. (2011) Regulation of horizontal gene transfer in *Bacillus subtilis* by activation of a conserved site-specific protease. *Journal of Bacteriology*, 193, 22–29.
- Bose, B., Auchtung, J.M., Lee, C.A. & Grossman, A.D. (2008) A conserved anti-repressor controls horizontal gene transfer by proteolysis. *Molecular Microbiology*, 70, 570–582.
- Botelho, J. & Schulenburg, H. (2021) The role of integrative and conjugative elements in antibiotic resistance evolution. *Trends in Microbiology*, 29, 8–18.
- Brophy, J.A.N., Triassi, A.J., Adams, B.L., Renberg, R.L., Stratis-Cullum, D.N., Grossman, A.D. et al. (2018) Engineered integrative and conjugative elements for efficient and inducible DNA transfer to undomesticated bacteria. *Nature Microbiology*, 3, 1043–1053.
- Burrus, V. & Waldor, M.K. (2004) Shaping bacterial genomes with integrative and conjugative elements. *Research in Microbiology*, 155, 376–386.
- Burrus, V., Pavlovic, G., Decaris, B. & Guédon, G. (2002) Conjugative transposons: the tip of the iceberg. *Molecular Microbiology*, 46, 601–610.
- Ciric, L., Jasni, A., de Vries, L.E., Agersø, Y., Mullany, P. & Roberts, A.P. (2013) The Tn916/Tn1545 family of conjugative transposons. In: *Madame Curie Bioscience Database [Internet]*. Landes Bioscience: Austin (TX), pp. 2000–2013. Available from: <https://www.ncbi.nlm.nih.gov/books/NBK63531/>
- Cury, J., Touchon, M. & Rocha, E.P.C. (2017) Integrative and conjugative elements and their hosts: composition, distribution and organization. *Nucleic Acids Research*, 45, 8943–8956.
- Decker, E.-M. (2001) The ability of direct fluorescence-based, two-colour assays to detect different physiological states of oral streptococci. *Letters in Applied Microbiology*, 33, 188–192.
- Decker, E.-M., Klein, C., Schwindt, D. & von Ohle, C. (2014) Metabolic activity of *Streptococcus mutans* biofilms and gene expression during exposure to xylitol and sucrose. *International Journal of Oral Science*, 6, 195–204.
- Delavat, F., Mitri, S., Pelet, S. & van der Meer, J.R. (2016) Highly variable individual donor cell fates characterize robust horizontal gene transfer of an integrative and conjugative element. *Proceedings of the National Academy of Sciences of the United States of America*, 113, E3375–E3383.
- DeWitt, T. & Grossman, A.D. (2014) The bifunctional cell wall hydrolase CwIT is needed for conjugation of the integrative and conjugative element ICEBs1 in *Bacillus subtilis* and *B. anthracis*. *Journal of Bacteriology*, 196, 1588–1596.
- Dimopoulou, I.D., Russell, J.E., Mohd-Zain, Z., Herbert, R. & Crook, D.W. (2002) Site-specific recombination with the chromosomal tRNA(Leu) gene by the large conjugative Haemophilus resistance plasmid. *Antimicrobial Agents and Chemotherapy*, 46, 1602–1603.
- Franke, A.E. & Clewell, D.B. (1981a) Evidence for conjugal transfer of a *Streptococcus faecalis* transposon (Tn916) from a chromosomal site in the absence of plasmid DNA. *Cold Spring Harbor Symposia on Quantitative Biology*, 45(Pt 1), 77–80.
- Franke, A.E. & Clewell, D.B. (1981b) Evidence for a chromosome-borne resistance transposon (Tn916) in *Streptococcus faecalis* that is capable of “conjugal” transfer in the absence of a conjugative plasmid. *Journal of Bacteriology*, 145, 494–502.
- Fronzes, R., Christie, P.J. & Waksman, G. (2009) The structural biology of type IV secretion systems. *Nature Reviews. Microbiology*, 7, 703–714.
- Fujimura-Kamada, K., Nouvet, F.J. & Michaelis, S. (1997) A novel membrane-associated metalloprotease, Ste24p, is required for the first step of NH2-terminal processing of the yeast a-factor precursor. *The Journal of Cell Biology*, 136, 271–285.
- Gibson, D.G., Young, L., Chuang, R.-Y., Venter, J.C., Hutchison, C.A., III & Smith, H.O. (2009) Enzymatic assembly of DNA molecules up to several hundred kilobases. *Nature Methods*, 6(343), 345.
- Gilchrist, C.L.M., Booth, T.J., van Wersch, B., van Grieken, L., Medema, M.H. & Chooi, Y.-H. (2021) Cblaster: a remote search tool for rapid identification and visualization of homologous gene clusters. *Bioinformatics Advances*, 1, vbab016.
- Gottesman, M.E. & Weisberg, R.A. (2004) Little lambda, who made thee? *Microbiology and Molecular Biology Reviews*, 68, 796–813.
- Grindley, N.D.F., Whiteson, K.L. & Rice, P.A. (2006) Mechanisms of site-specific recombination. *Annual Review of Biochemistry*, 75, 567–605.
- Guérout-Fleury, A.M., Frandsen, N. & Stragier, P. (1996) Plasmids for ectopic integration in *Bacillus subtilis*. *Gene*, 180, 57–61.
- Guglielmini, J., Quintais, L., Garcillán-Barcia, M.P., de la Cruz, F. & Rocha, E.P.C. (2011) The repertoire of ICE in prokaryotes underscores the unity, diversity, and ubiquity of conjugation. *PLoS Genetics*, 7, e1002222.
- Harwood, C.R. & Cutting, S.M. (1990) *Molecular biological methods for bacillus*. John Wiley & Sons. UK: Chichester.
- Hirano, N., Muroi, T., Takahashi, H. & Haruki, M. (2011) Site-specific recombinases as tools for heterologous gene integration. *Applied Microbiology and Biotechnology*, 92, 227–239.
- Iyer, L.M., Makarova, K.S., Koonin, E.V. & Aravind, L. (2004) Comparative genomics of the FtsK-HerA superfamily of pumping ATPases: implications for the origins of chromosome segregation, cell division and viral capsid packaging. *Nucleic Acids Research*, 32, 5260–5279.
- Jiang, X., Hall, A.B., Xavier, R.J. & Alm, E.J. (2019) Comprehensive analysis of chromosomal mobile genetic elements in the gut microbiome reveals phylum-level niche-adaptive gene pools. *PLoS One*, 14, e0223680.
- Johnson, C.M. & Grossman, A.D. (2014) Identification of host genes that affect acquisition of an integrative and conjugative element in *Bacillus subtilis*. *Molecular Microbiology*, 93, 1284–1301.
- Johnson, C.M. & Grossman, A.D. (2015) Integrative and conjugative elements (ICEs): what they do and how they work. *Annual Review of Genetics*, 49, 577–601.
- Jones, J.M., Grinberg, I., Eldar, A. & Grossman, A.D. (2021) A mobile genetic element increases bacterial host fitness by manipulating development. *eLife*, 10, e65924.
- King, S., Quick, A., King, K., Walker, A.R. & Shields, R.C. (2022) Activation of TnSmu1, an integrative and conjugative element, by an ImmR-like transcriptional regulator in *Streptococcus mutans*. *Microbiology (Reading)*, 168, 001254. Available from: <https://doi.org/10.1099/mic.0.001254>
- Koyanagi, S. & Lévesque, C.M. (2013) Characterization of a *Streptococcus mutans* intergenic region containing a small toxic

- peptide and its cis-encoded antisense small RNA antitoxin. *PLoS One*, 8, e54291.
- Lee, C.A. & Grossman, A.D. (2007) Identification of the origin of transfer (*oriT*) and DNA relaxase required for conjugation of the integrative and conjugative element ICEBs1 of *Bacillus subtilis*. *Journal of Bacteriology*, 189, 7254–7261.
- Lee, C.A., Auchtung, J.M., Monson, R.E. & Grossman, A.D. (2007) Identification and characterization of *int* (integrase), *xis* (excisionase) and chromosomal attachment sites of the integrative and conjugative element ICEBs1 of *Bacillus subtilis*. *Molecular Microbiology*, 66, 1356–1369.
- Lee, C.A., Babic, A. & Grossman, A.D. (2010) Autonomous plasmid-like replication of a conjugative transposon. *Molecular Microbiology*, 75, 268–279.
- Lee, C.A., Thomas, J. & Grossman, A.D. (2012) The *Bacillus subtilis* conjugative transposon ICEBs1 mobilizes plasmids lacking dedicated mobilization functions. *Journal of Bacteriology*, 194, 3165–3172.
- Lemon, K.P., Kurtser, I. & Grossman, A.D. (2001) Effects of replication termination mutants on chromosome partitioning in *Bacillus subtilis*. *Proceedings of the National Academy of Sciences of the United States of America*, 98, 212–217.
- Leonetti, C.T., Hamada, M.A., Laurer, S.J., Broulidakis, M.P., Swerdlow, K.J., Lee, C.A. et al. (2015) Critical components of the conjugation machinery of the integrative and conjugative element ICEBs1 of *Bacillus subtilis*. *Journal of Bacteriology*, 197, 2558–2567.
- Li, Y.-H., Lau, P.C.Y., Lee, J.H., Ellen, R.P. & Cvitkovitch, D.G. (2001) Natural genetic transformation of *Streptococcus mutans* growing in biofilms. *Journal of Bacteriology*, 183, 897–908.
- Lucchini, S., Desiere, F. & Brüssow, H. (1999) Similarly organized lysogeny modules in temperate *Siphoviridae* from low GC content gram-positive bacteria. *Virology*, 263, 427–435.
- Lunde, T.M., Hjerde, E. & Al-Haroni, M. (2021) Prevalence, diversity and transferability of the Tn916–Tn1545 family ICE in oral streptococci. *Journal of Oral Microbiology*, 13, 1896874.
- Mashburn-Warren, L., Morrison, D.A. & Federle, M.J. (2010) A novel double-tryptophan peptide pheromone is conserved in mutants and pyogenic streptococci and controls competence in *Streptococcus mutans* via an Rgg regulator. *Molecular Microbiology*, 78, 589–606.
- Miyazaki, R. & van der Meer, J.R. (2013) A new large DNA fragment delivery system based on integrase activity from an integrative and conjugative element. *Applied and Environmental Microbiology*, 79, 4440–4447.
- Narasimhan, G., Bu, C., Gao, Y., Wang, X., Xu, N. & Mathee, K. (2002) Mining protein sequences for motifs. *Journal of Computational Biology*, 9, 707–720.
- Needleman, S.B. & Wunsch, C.D. (1970) A general method applicable to the search for similarities in the amino acid sequence of two proteins. *Journal of Molecular Biology*, 48, 443–453.
- Nomura, R., Matayoshi, S., Otsugu, M., Kitamura, T., Teramoto, N. & Nakano, K. (2020) Contribution of severe dental caries induced by *Streptococcus mutans* to the pathogenicity of infective endocarditis. *Infection and Immunity*, 88, e00897–19.
- Olsen, I., Tribble, G.D., Fiehn, N.-E. & Wang, B.-Y. (2013) Bacterial sex in dental plaque. *Journal of Oral Microbiology*, 5, 20736. Available from: <https://doi.org/10.3402/jom.v5i0.20736>
- Oppenheim, A.B., Kobilier, O., Stavans, J., Court, D.L. & Adhya, S. (2005) Switches in bacteriophage lambda development. *Annual Review of Genetics*, 39, 409–429.
- Pembroke, J.T. & Stevens, E. (1984) The effect of plasmid R391 and other IncJ plasmids on the survival of *Escherichia coli* after UV irradiation. *Journal of General Microbiology*, 130, 1839–1844.
- Peters, J.M., Koo, B.-M., Patino, R., Heussler, G.E., Hearne, C.C., Qu, J. et al. (2019) Enabling genetic analysis of diverse bacteria with Mobile-CRISPRi. *Nature Microbiology*, 4, 244–250.
- Petersen, F.C. & Scheie, A.A. (2010) Natural transformation of oral streptococci. In: Seymour, G.J., Cullinan, M.P. & Heng, N.C.K. (Eds.) *Oral biology: molecular techniques and applications*. Totowa, NJ: Humana Press, pp. 167–180. Available from: https://doi.org/10.1007/978-1-60761-820-1_12
- Petit, M.-A., Dervyn, E., Rose, M., Entian, K.-D., McGovern, S., Ehrlich, S.D. et al. (1998) PcrA is an essential DNA helicase of *Bacillus subtilis* fulfilling functions both in repair and rolling-circle replication. *Molecular Microbiology*, 29, 261–273.
- Pfaffl, M.W. (2001) A new mathematical model for relative quantification in real-time RT-PCR. *Nucleic Acids Research*, 29, e45.
- Reck, M. & Wagner-Döbler, I. (2016) Carolacton treatment causes delocalization of the cell division proteins PknB and DivIVA in *Streptococcus mutans* in vivo. *Frontiers in Microbiology*, 7, 684.
- Reinhard, F., Miyazaki, R., Pradervand, N. & van der Meer, J.R. (2013) Cell differentiation to “mating bodies” induced by an integrating and conjugative element in free-living bacteria. *Current Biology*, 23, 255–259.
- Rice, P., Longden, I. & Bleasby, A. (2000) EMBOSS: the European molecular biology open software suite. *Trends in Genetics*, 16, 276–277.
- Roberts, A.P. & Mullany, P. (2009) A modular master on the move: the Tn916 family of mobile genetic elements. *Trends in Microbiology*, 17, 251–258.
- Roberts, A.P. & Mullany, P. (2011) Tn916-like genetic elements: a diverse group of modular mobile elements conferring antibiotic resistance. *FEMS Microbiology Reviews*, 35, 856–871.
- Roberts, A.P., Pratten, J., Wilson, M. & Mullany, P. (1999) Transfer of a conjugative transposon, Tn5397 in a model oral biofilm. *FEMS Microbiology Letters*, 177, 63–66.
- Roberts, A.P., Cheah, G., Ready, D., Pratten, J., Wilson, M. & Mullany, P. (2001) Transfer of Tn916-like elements in microcosm dental plaques. *Antimicrobial Agents and Chemotherapy*, 45, 2943–2946.
- Rocco, J.M. & Churchward, G. (2006) The integrase of the conjugative transposon Tn916 directs strand- and sequence-specific cleavage of the origin of conjugal transfer, *oriT*, by the endonuclease Orf20. *Journal of Bacteriology*, 188, 2207–2213.
- San Millan, A. & MacLean, R.C. (2017) Fitness costs of plasmids: a limit to plasmid transmission. *Microbiol Spectr*, 5, 5.5.02.
- Santoro, F., Vianna, M.E. & Roberts, A.P. (2014) Variation on a theme; an overview of the Tn916/Tn1545 family of mobile genetic elements in the oral and nasopharyngeal streptococci. *Frontiers in Microbiology*, 5, 535.
- Schindelin, J., Arganda-Carreras, I., Frise, E., Kaynig, V., Longair, M., Pietzsch, T. et al. (2012) Fiji: an open-source platform for biological-image analysis. *Nature Methods*, 9, 676–682.
- Serfiotis-Mitsa, D., Roberts, G.A., Cooper, L.P., White, J.H., Nutley, M., Cooper, A. et al. (2008) The Orf18 gene product from conjugative transposon Tn916 is an ArdA antirestriction protein that inhibits type I DNA restriction-modification systems. *Journal of Molecular Biology*, 383, 970–981.
- Shanker, E. & Federle, M.J. (2017) Quorum sensing regulation of competence and bacteriocins in *Streptococcus pneumoniae* and *mutans*. *Genes*, 8, 15.
- Shields, R.C., Zeng, L., Culp, D.J. & Burne, R.A. (2018) Genomewide identification of essential genes and fitness determinants of *Streptococcus mutans* UA159. *mSphere*, 3, e00031–18.
- Son, M., Ahn, S.-J., Guo, Q., Burne, R.A. & Hagen, S.J. (2012) Microfluidic study of competence regulation in *Streptococcus mutans*: environmental inputs modulate bimodal and unimodal expression of *comX*. *Molecular Microbiology*, 86, 258–272.
- Thomas, J., Lee, C.A. & Grossman, A.D. (2013) A conserved helicase processivity factor is needed for conjugation and replication of an integrative and conjugative element. *PLoS Genetics*, 9, e1003198.
- Wecke, J., Madela, K. & Fischer, W. (1997) The absence of D-alanine from lipoteichoic acid and wall teichoic acid alters surface charge, enhances autolysis and increases susceptibility to methicillin in *Bacillus subtilis*. *Microbiology*, 143, 2953–2960.

- Wozniak, R.A.F. & Waldor, M.K. (2010) Integrative and conjugative elements: mosaic mobile genetic elements enabling dynamic lateral gene flow. *Nature Reviews. Microbiology*, 8, 552–563.
- Wright, L.D. & Grossman, A.D. (2016) Autonomous replication of the conjugative transposon Tn916. *Journal of Bacteriology*, 198, 3355–3366.
- Xiang, Y., Morais, M.C., Cohen, D.N., Bowman, V.D., Anderson, D.L. & Rossmann, M.G. (2008) Crystal and cryoEM structural studies of a cell wall degrading enzyme in the bacteriophage phi29 tail. *Proceedings of the National Academy of Sciences of the United States of America*, 105, 9552–9557.
- Xie, Z., Okinaga, T., Qi, F., Zhang, Z. & Merritt, J. (2011) Cloning-independent and counterselectable markerless mutagenesis system in *Streptococcus mutans*. *Applied and Environmental Microbiology*, 77, 8025–8033.
- Zhang, K., Ou, M., Wang, W. & Ling, J. (2009) Effects of quorum sensing on cell viability in *Streptococcus mutans* biofilm formation. *Biochemical and Biophysical Research Communications*, 379, 933–938.

SUPPORTING INFORMATION

Additional supporting information can be found online in the Supporting Information section at the end of this article.

How to cite this article: McLellan, L. K., Anderson, M. E. & Grossman, A. D. (2022). TnSmu1 is a functional integrative and conjugative element in *Streptococcus mutans* that when expressed causes growth arrest of host bacteria. *Molecular Microbiology*, 00, 1–18. <https://doi.org/10.1111/mmi.14992>